ADAPTATION TO GLUCOSE DEPRIVATION IN 3T3-L1 ADIPOCYTES

By

MAXINE FISHER

A DISSERTATION PRESENTED TO THE GRADUATE SCHOOL
OF THE UNIVERSITY OF FLORIDA IN PARTIAL FULFILLMENT
OF THE REQUIREMENTS FOR THE DEGREE OF
DOCTOR OF PHILOSOPHY

UNIVERSITY OF FLORIDA

1998

I dedicate this work to my father, the late Maximillian O. Fisher.

ACKNOWLEDGMENTS

I am indebted to the members of my committee, Drs. Brian Cain, Michael Kilberg, Daniel Purich, Bruce Stevens, and my advisor Susan Frost, for their sincere interest in my success as a scientist. I was fortunate to have worked with Dr. Bob McMahon and benefitted from his knowledge and friendship. Many other friends have enriched my experience in graduate school. Dr. Edi Zhang, Jane Mellott, and Kelly McDonald have given me understanding, compassion, and cheer. Greg Bloom and Chris Davis have been supportive, generous, and absolutely hilarious. I also thank Mike Waters, Dr. Catherine Golden, and Dr. Tiffany Alley for their friendship and wisdom--their candor and levelheadedness have inspired me. Finally, I am extremely grateful for my mother and four brothers whose encouragement and love will always give me strength.

TABLE OF CONTENTS

ACKNOWLEDGMENTS iii

LIST OF TABLES vii

LIST OF FIGURES viii

ABSTRACT xi

CHAPTERS

1 OVERVIEW. 1

  Introduction 1
    The Glucose Transporter Family. 2
    GLUT1, the Constitutive Glucose Transporter 4
    Regulation of Glucose Transport by Glucose. . 5
    Glucose Deprivation in 3T3-L1 Adipocytes. . . 8
    Possible Mechanisms for Glucose Deprivation-induced Transport Activation 10

2 MATERIALS AND METHODS 17

  Materials 17
  Methods 18
    Cell Culture and Glucose Deprivation 18
    Whole Cell Glucose Transport 20
    Subcellular Fractionation of 3T3-L1 Adipocytes 22
    Electron Microscopy 25
    Markwell Assay for Protein Determination . . . 25
    Gel Electrophoresis 27
      One-dimensional gel electrophoresis . . . 27
      Two-dimensional gel electrophoresis . . . 27
    Electrotransfer and Immunoblotting 29
    RNA Isolation and Northern Analysis 30
    Plasma Membrane Vesicle Transport 31
    Cell Surface Biotinylation 32

Isolation of GLUT1-Containing Vesicles 35
Metabolic Radiolabeling of 3T3-L1 Adipocytes . 37
Preparation of Protein for Microsequencing . . 38
Concentration of glucose-dependent protein 38
Microsequencing of glucose-dependent protein 40
Detergent Extraction of Proteins 41

3 EFFECT OF GLUCOSE DEPRIVATION ON GLUCOSE TRANSPORT AND TRANSPORTER DISTRIBUTION IN 3T3-L1 ADIPOCYTES 43

Introduction 43
Results 45
Effect of Glucose Deprivation on Uptake of [^{3}H]2-deoxyglucose 45
Subcellular Fractionation in 3T3-L1 Adipocytes 47
Distribution of GLUT1 and GLUT4 57
Plasma Membrane Vesicle Transport 58
Conclusions 61

4 EVIDENCE FOR PARTICIPATION OF A LABILE PROTEIN IN GLUCOSE TRANSPORT ACTIVATION 64

Introduction 64
Results 67
Effect of Inhibitors of Protein Degradation on Glucose Transport in Control, Glucose-deprived, and Glucose-refed 3T3-L1 Adipocytes 67
Response of Enhanced Transport Activity to Glucose Readdition in Glucose-deprived 3T3-L1 Adipocytes 70
Effect of Tunicamycin on Glucose Transport in Control and Glucose-deprived 3T3-L1 Adipocytes 73
Analysis of Proteins in Subcellular Fractions from Control and Glucose-deprived 3T3-L1 Adipocytes 79
Conclusions 81

5 IDENTIFICATION AND CHARACTERIZATION OF GLUCOSE-DEPENDENT PROTEINS 86

Introduction 86
Results 88

Metabolically Labeled Membrane Proteins from Glucose-fed and Glucose-deprived 3T3-L1 Adipocytes 88
Isolation, Concentration, and Microsequencing of a Glucose-dependent Membrane Protein 95
Immunoblotting Studies 96
Anti-vimentin studies 98
Peptide synthesis from glucose-dependent protein sequence data 98
Membrane Association of Glucose-dependent Proteins 99
One-dimensional gel electrophoresis . . 100
Two-dimensional gel electrophoresis . . 102
Effect of Glucose Refeeding on Glucose-dependent Proteins 104
Subcellular Localization of Glucose-dependent Proteins 107
Conclusions 107

6 CONCLUSIONS AND FUTURE DIRECTIONS 112

Conclusions 112
Future Directions 119

APPENDICES

I CHARACTERIZATION OF GLUCOSE TRANSPORT IN HUMAN PULMONARY AORTIC ENDOTHELIAL CELLS 124

II PRELIMINARY EXPERIMENTS 136

Other Inhibitors of Protein Degradation 136

LIST OF REFERENCES 140

BIOGRAPHICAL SKETCH. 146

LIST OF TABLES

Table page

3-1 - Protein Recovery from Subcellular Fractionation . . 49

3-2 - Subcellular Distribution of GLUT1 and GLUT4 53

5-1 - Comparison of Densitometric Values for Selected Spots 93

AI-1- Effect of Glucose Deprivation on Transport Kinetics in HPAE Cells 131

AI-2- Ratio of Glucose-deprived/Glucose-fed Km and Vmax Values from Table AI-1 131

LIST OF FIGURES

Figure page

2-1 - Subfractionation of 3T3-L1 Adipocytes 24

2-2 - Isolation and Concentration of Glucose-dependent Protein 39

3-1 - Effect of Glucose Deprivation on Uptake of [^{3}H]2-deoxyglucose 46

3-2 - Effect of Clearance Size on Subfractionation . . . 48

3-3 - Distribution of Cell-surface Biotinylated Proteins 50

3-4 - Subcellular Distribution of GLUT1 and GLUT4 52

3-5 - Electron Micrographs of Membrane Fractions 54

3-6 - Orientation of Vesicles from Subcellular Fractions 55

3-7 - Effect of Glucose-deprivation on Glucose Uptake in Plasma Membrane Vesicles 60

4-1 - Glucose Refeeding +/- Chloroquine 69

4-2 - Response of Enhanced Transport Activation to Glucose Readdition in Control and Glucose-deprived 3T3-L1 adipocytes 72

4-3 - Effect of Tunicamycin on Glucose Transport Activity in Glucose-fed and Glucose-deprived 3T3-L1 Adipocytes 74

4-4 - Subfractionation of Glucose-fed versus Glucose-deprived +/- Tunicamycin-treated 3T3-L1 Adipocytes 76

4-5 - Densitometric Analysis of Plasma Membrane Fractions from Figure 4-4 78

5-1 - Synthesis of Glucose-deprived vs. Fed Proteins . . 89

5-2 - Spots Selected for Densitometric Comparison 91

5-3 - Assignment of Spots Selected for Densitometric Analysis 92

5-4 - Densitometric Ratio of Selected Spots 94

5-5 - Results of Sequence Analysis on 50 kDa Protein . . 97

5-6 - Triton X-100 Extraction of 3T3-L1 Adipocytes . . 101

5-7 - NP40 Insoluble Fraction from Metabolically Labeled 3T3-L1 Adipocytes 103

5-8 - Anti-vimentin Immunoblot on NP40 Insoluble Fraction from 3T3-L1 Adipocytes 105

5-9 - NP40 Insoluble Fraction from Metabolically labeled Glucose-fed, Glucose-deprived, and Glucose-refed 3T3-L1 Adipocytes 106

5-10- Plasma Membrane Fraction of Glucose-fed and Glucose-deprived Metabolically Labeled 3T3-L1 Adipocytes 108

6-1 - Model of Response to Glucose Deprivation in 3T3-L1 Adipocytes 118

6-2 - Isolation of GLUT1-containing Vesicles Using Magnetic beads 122

AI-1 -Linearity of Glucose Uptake in Human Pulmonary Aortic Endothelial Cells 126

AI-2 -Kinetics of Glucose Transport in HPAE Cells . . . 127

AI-3 - Effect of Glucose Deprivation on Uptake of $[^3H]$2-deoxyglucose in Human Pulmonary Aortic Endothelial Cells 128

AI-4 - Effect of Glucose Deprivation on Transport Kinetics in HPAE cells 130

AI-5 - Effect of Chronic Glucose on Transport in HPAEs 133

AI-6 - Effect of Protein and mRNA Synthesis Inhibitors on Glucose Transport in HPAE Cells 134

AI-7 - Effect of Glucose Deprivation on Levels of GLUT1 protein and mRNA in HPAE Cells ± Cycloheximide or Actinomycin D 135

AII-1- Effect of Leupeptin on Reversal of Transport Activation in 3T3-L1 Adipocytes 138

AII-2- Effect of Lactacystin on Reversal of Transport Activation in 3T3-L1 Adipocytes. . . . 139

Abstract of Dissertation Presented to the Graduate School
of the University of Florida in Partial Fulfillment of the
Requirements for the Degree of Doctor of Philosophy

ADAPTATION TO GLUCOSE DEPRIVATION IN 3T3-L1 ADIPOCYTES

By

Maxine Fisher

May, 1998

Chairperson: Susan C. Frost
Major Department: Biochemistry and Molecular Biology

The phenomenon of glucose transport activation in response to glucose deprivation was studied in 3T3-L1 adipocytes. This effect is dependent on new protein synthesis. We carried out glucose deprivation in the presence of fructose, which provided cells with a source of carbohydrate and interfered little with the observed 8- to 10-fold transport activation. A novel procedure for the subfraction of 3T3-L1 adipocytes was used to rule out the involvement of translocation in transport activation. We established this protocol to study the subcellular distribution of the two glucose transporters present in 3T3-L1 adipocytes, GLUT1 and GLUT4. GLUT1 was shown to be the major transporter at the cell surface. Glucose deprivation did not alter the level of either transporter at the cell surface, with 20% of GLUT1 and 3% of GLUT4 appearing at the plasma membrane in both control and glucose-deprived cells. We also showed that plasma membranes of glucose-deprived cells retained transport activity. Plasma membrane proteins were then analyzed using the techniques of cell surface biotinylation and our novel subfractionation procedure. In addition, newly synthesized proteins from total membrane preparations were analyzed by two-dimensional gel electrophoresis using metabolic radiolabeling. We studied adaptation to glucose deprivation with addition of glycosylation and protein degradation inhibitors and with glucose re-feeding experiments. Tunicamycin diminished the activation response by 50%. Re-addition of glucose to deprived cells returned transport levels to basal within 4 hours. This was unaffected by inhibition of protein degradation. Transport activation was twice as fast in glucose deprived then refed cells compared with fed controls. Novel proteins were synthesized during glucose deprivation. One glucose-dependent protein (50 kDa, pI 5.2) was isolated and microsequenced which resulted in some sequence that was novel and some that matched the intermediate filament protein vimentin. Unlike vimentin which by immunoblotting was shown not to change in response to glucose deprivation, we observed that this 50 kDa protein appeared with glucose withdrawal and disappeared with glucose refeeding. This protein and at least one other which requires future study are implicated in adaptation of 3T3-L1 adipocytes to glucose deprivation.

CHAPTER 1
OVERVIEW

Introduction

The ability of a cell to respond to its environment is crucial to its survival and the elucidation of the mechanisms behind such regulation is an important area of research. All living cells must exhibit a capacity to select for the absorption of certain molecular species across the membrane. They do so by providing specific transport proteins which overcome the barrier of the lipid bilayer. Molecules which traverse the membrane from low concentration to high concentration do so via active transport. The energy from an exergonic reaction, often the hydrolysis of ATP, is required for active transport to become favorable (1). Certain transport proteins, or transporters, allow molecules to move down their concentration gradient. This is called facilitated transport. The facilitated transport of glucose into mammalian cells has been studied for fifty years in the case of the human erythrocyte glucose transport system (2). The ongoing research has resulted in the identification of a family of proteins responsible for facilitated glucose transport in mammalian cells, discussed in the following section.

The Glucose Transporter Family

Of the multitude of ions and molecules that are able to traverse cell membranes, glucose is extremely important because it serves as the main fuel for most cells. Cells meet their need with the facilitated transport of glucose across the membrane. With the application of molecular biology techniques, researchers have discovered that a family of structurally related proteins is responsible for the facilitated transport of glucose (3). The GLUT (for GLUcose Transporter) family of transporters were named in order of their discovery. GLUT1 was purified from erythrocytes, GLUT2 from liver, GLUT3 from brain, GLUT4 from muscle and fat, GLUT5 (a proposed fructose transporter) from small intestine, GLUT6 was found to be a pseudogene, and GLUT7 isolated from liver endoplasmic reticulum (for a recent review, see (4)). Kinetic analyses of the equilibrium exchange values of each isoform for the glucose analogue 3-O-methyl-D-glucose indicate that the existence of multiple glucose transporter isoforms may reflect diversity in the metabolic needs of various tissues. The K_m values are about 20 mM for GLUT1, 42 mM for GLUT2, 10 mM for GLUT3, and 2 mM for GLUT4 (5). This family of transporters has been under extensive investigation because they represent a key point for control of glucose metabolism.

The first four transporters in the GLUT family have been found in more than one cell type. GLUT1 was purified from erythrocytes where it comprises about 5% of the membrane protein (6) and later cloned (7). This protein, known as the constitutive glucose transporter, is found in many tissues and cells including brain, placenta, muscle and fat (for review, see (8)). The liver-type transporter, GLUT2, is also found in pancreatic β-cells and basolateral membranes of kidney proximal tubules and small intestine. A rationale has been proposed for the high Km of this transporter. The tissues expressing GLUT2 mentioned above are involved in release of glucose during fasting, glucose sensing and transepithelial glucose transport, respectively. The high Km allows glucose flux to change in a linear fashion with physiological intra- and extracellular glucose concentrations. GLUT3 was determined to be expressed in tissues with a high glucose demand, such as brain and nerve and has been proposed to act together with GLUT1 to meet this high energy requirement. The increase in glucose transport which results from insulin stimulation was shown to occur by translocation (9;10). The intense interest in insulin-responsiveness led to the cloning of GLUT4 by five independent groups (11-15). The signalling pathway between insulin, the insulin receptor, and GLUT4 translocation remains to be elucidated. Gould and Holman (8) suggest that each of the transporters in the GLUT family has its own role in the regulation of whole-body homeostasis.

Hydropathy plots of sequence data suggest that the members of the GLUT family contain twelve membrane spanning domains with both the amino and carboxy termini facing the cytoplasm (2). Each has a large extracellular loop between the first two membrane spanning helices. Also, there is a large intracellular loop between membrane spanning helices 6 and 7. The proteins in the GLUT family exhibit overall homology within species ranging from 54 to 65% with the most identity in the membrane spanning domains and the least in the large cytoplasmic regions (16). This divergence in the - and C-terminal domains has led to the hypothesis that these areas contain sorting and targeting information (17).

GLUT1, the Constitutive Glucose Transporter

Much of the early work on glucose transport was done on the erythrocyte type or GLUT1 transporter due to its abundance in red blood cells (18). Subsequent studies showed that most mammalian cells express GLUT1 mRNA which encodes for the GLUT1 protein with a molecular weight range of 45 to 55 kDa. Transformation of cell culture lines has been generally observed to result in elevation of GLUT1 protein and mRNA levels (8). Differences in the molecular weight of GLUT1 from different tissues may result from oligosaccharide heterogeneity (3). There is one consensus site available for N-linked glycosylation on the extracellular loop between the first two transmembrane helices in GLUT1. Although the site-directed mutagenesis studies (mentioned below) suggest that only a few amino acids are obligatory for function, there is 98% sequence identity between human and rat GLUT1 proteins (3), exemplifying a high degree of conservation. Clearly, glucose transport, in particular that mediated by GLUT1, is essential in most mammalian cells. Understanding the mechanisms behind regulation of GLUT1, a conserved and ubiquitous protein, could have broad ramifications.

Regulation of Glucose Transport by Glucose

Nutrient control of gene and protein expression is a topic of ongoing study in mammalian cells. In particular, the ability of certain nutrients to control their own metabolism is of great importance. Reviews in this area include those concerning cholesterol and carbohydrate metabolism (19), and amino acid transport (20). In addition, the many studies regarding glucose-dependent gene transcription (17) and glucose transporter regulation (21) have been recently reviewed. The focus of our laboratory has been regulation of glucose transport. The goal of this research is to identify elements of the adaptation response in cells specifically to glucose withdrawal.

Many studies have been performed investigating the effect of glucose on expression of glucose transporters (21). Of particular interest in these studies are the insulin-sensitive tissues. The work has been carried out in either diabetic animal models or cultured cells. Klip et al. (21) emphasize that *(I)* cells in culture have an advantage experimentally over animal models and *(ii)* different mechanisms exist for the control of glucose transport by glucose in different cell types. The major benefit of using cultured cells is that they allow the manipulation of glucose levels without the effects of the hormonal and metabolic changes which would occur *in vivo*. There are several examples of different means of glucose regulation of transport in cultured cells. The studies have made use of glucose deprivation to examine transporter regulation.

In non-insulin-responsive cells, GLUT4 is not expressed. Glucose deprivation of normal rat kidney fibroblasts resulted in increased glucose transport and translocation of GLUT1 to the plasma membrane (22) GLUT1 mRNA, however, was not affected. Interestingly, transport, GLUT1 protein, and GLUT1 mRNA did not change with glucose deprivation of bovine vascular endothelial cells (23). With 3T3-C2 fibroblasts investigators observed increased glucose transport and GLUT1 protein levels with no change in GLUT1 mRNA (24). The mechanism in this case was increased protein stability. In rat brain glial and neuronal cultures, glucose deprivation increased glucose transport (25). GLUT1 mRNA and protein both increased in glial cells but did not change in neuronal cells. An increase in GLUT1 mRNA and protein were observed when bovine brain microvessel endothelial cells were glucose-deprived (26). Using nuclear run-on analysis, the mechanism was determined to be increased mRNA stability as opposed to an increase in mRNA synthesis. The non-insulin-responsive cells discussed here exhibited diverse responses to glucose deprivation.

Insulin-responsive cells also demonstrate type-specific responses to glucose deprivation. L6 myotubes responded to glucose deprivation with increased transport followed by increased GLUT mRNA then protein levels (25). BC3H1 myocytes increased both GLUT1 protein and mRNA levels to a greater extent than transport upon glucose deprivation (27). In contrast, primary cultures of fetal muscle showed a similar increase in both GLUT1 mRNA and protein with glucose deprivation (28). Again, these studies indicate the distinct ways in which different cell types respond to glucose deprivation. However, GLUT1 appears to be a common factor in response of cells to glucose deprivation.

Glucose Deprivation in 3T3-L1 Adipocytes

One cell type expressing GLUT1 which is of considerable importance in the study of glucose transport is the adipocyte, primarily because of its insulin-responsiveness. Adipose tissue, along with cardiac and skeletal muscle, express GLUT4, the insulin-responsive transporter. The increase in the rate of glucose transport in adipocytes in response to an acute insulin challenge is due in large part to the translocation of the GLUT4 transporter from an intracellular vesicular pool to the plasma membrane (9;10). The GLUT1 transporter also undergoes insulin-stimulated translocation but only to a fraction of the extent of that seen for GLUT4 (29). Because isolated adipocytes have a limited time of viability, the cell line known as 3T3-L1 adipocytes was developed from mouse embryo fibroblasts (30) and has proved invaluable for long-term experiments to evaluate regulation of glucose transport.

The 3T3-L1 adipocyte cell line offers a good model for the study of nutrient control. For example, one condition that regulates the rate of glucose transport in 3T3-L1 cells is glucose deprivation (31-33). Although this phenomenon has been documented in numerous other cell types, it is clear from these studies that different cell types utilize different mechanisms to increase glucose transport (for review, see(21)). For example, an increase in GLUT1 mRNA has been shown in chick embryo fibroblasts (34), glia (35), myocytes (27) and L6 muscle cells (25). However in normal rat kidney fibroblasts (22), transport increases via GLUT1 translocation, with no change in GLUT1 mRNA. The elevated transport rate observed in the study by van Putten and Krans (31) was defined as an increase in the number of transporters or their intrinsic activity. Protein synthesis was also determined to be required for the increase in glucose uptake. Our laboratory and others have confirmed these results (22) (31;36).

Glucose deprivation drives the synthesis of a second glycoform of GLUT1 which migrates further on SDS PAGE (p37) than gels than the normal glycoform (p45). Although a 10-fold increase in glucose transport activity was seen in response to glucose deprivation, GLUT1 protein levels did not coincide with transport activity, that is, the level of normal glycoform did not change. The appearance of the lower molecular weight glycoform contributed to a 2-fold increase in total GLUT1 protein with extended deprivation. This protein is unlikely to be responsible for the glucose deprivation-induced increase in activity because *(I)*, the increase in transport activity precedes the appearance of this glycoform, and *(ii)* lower concentrations of extracellular glucose are required to observe this protein than are needed for increased uptake (36). A two- to three-fold increase in cell-surface GLUT1 reported by Kozka et al. (37) also does not account for the observed elevation in transport.

Possible Mechanisms for Glucose Deprivation-induced Transport Activation

The mechanisms for the up-regulation of glucose transport in response to glucose deprivation are not clear. However, there are many possibilities. The glucose molecule itself is one of the elements responsible for modulating the transporter as shown by the ability of 3-O-methyl glucose (a non-metabolizable sugar) to both block and reverse the increase in uptake. One manner in which glucose could have such an effect is through altering the conformation of the transporter. Transport is generally thought to occur via a conformational change in the transporter which alternately presents the substrate binding site at the exo- or endofacial sides of the membrane (2). A possibility for regulation is the existence of modifier sites on the transporter which when occupied could accelerate the reorientation of the transporter, leading to an increase in uptake (18).

Using molecular modeling and molecular dynamics techniques Gould and Holman (8) studied the conformational flexibility of the glucose transporter. These investigators found that the tenth transmembrane helix is capable of large conformational changes and that it may be responsible for the alternate substrate binding site presentation. Other studies have examined the sequence of the transporter for impact on conformation. The role of prolines in transmembrane helices had previously been studied and categorized as having structural or dynamic effects (38). Tamori et al. (39) examined the effect of mutation of proline 385, which is highly conserved in the tenth transmembrane helix, on glucose transport. These authors suggest that Pro 385 functions in presenting the outward facing conformation since substituting isoleucine at this position reduced transport activity and prevented the transporter from being labeled by exofacial ligands by reducing conformational flexibility. In another study, these authors found that a tyrosine 293 to isoleucine GLUT1 mutant is fixed in an outward facing conformation (40).

The deprivation-induced elevation of glucose transport requires protein synthesis. An unidentified protein, whose action or expression is glucose dependent could modulate the system by affecting the orientation of the transporter. A protein involved in regulation of glucose transport could potentially act either by binding glucose or the transporter. Studies have been done which demonstrate the existence of proteins capable of each type of interaction. First, there have been reports of proteins that bind glucose. Lipmann and Lee (41) were interested in the increase in glucose uptake observed upon malignant transformation of cells, specifically, chicken fibroblasts. They isolated a glucose binding factor using affinity chromatography. Experiments were done showing that the factor is more abundant in transformed cells than in normal cells, that it increases glucose uptake in quiescent cells, and that its effect on glucose uptake is comparable to that of insulin (41).

Another example of a ligand binding protein is the periplasmic glucose/galactose binding protein from *Salmonella typhimurium* which has been extensively studied. This is a soluble protein located in the periplasm of Gram-negative bacteria. Its mode of action may be indicative of the mammalian mechanism for transport regulation. After directly binding the ligand (glucose/galactose), these receptors become activated and recognized by the membrane receptor for chemotaxis. The crystal structure of this protein has been determined at a resolution of 1.9 angstroms (42), which may prove useful with respect to mammalian systems regarding the sequence or arrangement of glucose binding motifs. In *Saccharomyces cerevisiae* unusual glucose transporters have been implicated as glucose sensors. Snf3p is necessary for the induction of several hexose transporter genes by low glucose levels. Rgt2p appears to be a high glucose sensing counterpart to Snf3p. The authors suggest that acting as glucose receptors, these proteins recognize levels of glucose. The proteins then generate an intracellular glucose signal which induces the required genes (43).

The alternative viewpoint is that transport can be regulated by a protein which associates with the transporter directly. Proteins which bind the glucose transporter have been reported (44;45) which led to the hypothesis that the glucose transporter indirectly regulates glucose utilization. To determine if the GLUT1 transporter from human erythrocytes interacts with any cytosolic proteins (such as enzymes involved in the glycolytic pathway) these investigators incubated human erythrocyte hemolysate with purified human erythrocyte glucose transporter vesicles. This group observed many proteins that associated with the glucose transporter and reported a specific association with glyceraldehyde-3-phosphate dehydrogenase (44) and glucokinase (45). A protein could also modify glucose transport activity by association with the vesicular compartment in which the transporter resides. Examples of proteins which increase transport exist. Veyhl et al. (46) cloned a plasma membrane-associated protein (RS1) which alters the expression of the Na^+-D-glucose cotransporter. Their data suggest that the cotransporter contains a regulatory subunit which is identical or homologous to RS1. Also, proteins in the rBAT/4F2hc family have been cloned. These proteins have been shown to increase transport of specific neutral and positively charged amino acids upon injection of their cRNAs into *Xenopus* oocytes (for review see, (20)).

Potential regulatory proteins can be detected even when the glucose transporter is present in low abundance. Two studies presented strategies for characterizing proteins in GLUT4 vesicles with the hope of identifying proteins involved in the regulation of GLUT4 by insulin (47;48). Using isolated rat adipocytes, in which GLUT4 is of low abundance, Kandror and Pilch (48) labeled recyclable proteins first by cell-surface biotinylation and followed this with immunoadsorption of GLUT4-containing vesicles. These authors reported Triton X-100-resistant and soluble fractions from these vesicles. They described a novel 160 kDa protein in the Triton-soluble fraction (actually one of three proteins in that fraction) which cycled between the cell surface and intracellular location, identically to GLUT4(48). Mastick et al. (47) used an approach similar to that of Kandror and Pilch and independently reported the same previously undescribed protein. Once isolated, the 160 kDa protein was found to have sequence similarity to amidotransferase (49;50).

My research presents evidence for the participation of a protein other than GLUT1 in enhanced transport induced by glucose deprivation. Using a technique which allows effective subfractionation of 3T3-L1 adipocytes, we show that GLUT1 levels do not change at the cell surface with glucose deprivation. We also show that GLUT4 is not responsible for this process. With protein synthesis and degradation inhibitors, we offer indirect evidence of a protein(s) involved in transport activation. In addition, we show the appearance of newly synthesized membrane proteins in response to glucose deprivation. These proteins are part of the adaptation response of 3T3-L1 adipocytes to glucose deprivation. Once antibodies are available to these proteins, direct tests for their role in transport activation will be possible. We discuss potential methods for this, in addition to presenting a technique for the isolation of GLUT1-containing vesicles. This technique, in combination with the subfractionation protocol, will allow colocalization studies using antibodies to glucose-dependent proteins and are likely to be instructive in future studies as to the mechanism underlying transport activation.

CHAPTER 2
MATERIALS AND METHODS

Materials

Dulbecco's modified Eagle's medium (DMEM) and glucose-free DMEM were purchased from Life Technologies, Inc (Gaithersburg, MD). Cysteine-, methionine-, and glucose-free DMEM was made according to Dulbecco and Freeman (51) excluding those components. M199 medium was acquired from Sigma (St. Louis, MO). Calf serum (lot number J13605) and fetal bovine serum (lot number LB95508) were obtained from Intergen (Purchase, NY). To remove glucose, fetal bovine serum (FBS) was dialyzed against phosphate buffered saline solution, pH 7.4 (PBS) over 48 hours using dialysis tubing (SpectraPor) with a molecular weight cutoff of 13,000. Rabbit polyclonal antibodies for GLUT1 and GLUT4 were generated against synthetic fragments composed of the C-terminal 13 amino acids, respectively. Anti-GRP78 was made against a peptide containing the first 12 residues in the N terminus. Anti-sialyltransferase and anti-Na^+,K^+-ATPase were gifts from Dr. William Dunn (University of Florida) and

Dr. Michael Caplan (Yale University), respectively. The cDNA for the GLUT1 probe was a gift from Dr. Maureen Charron (Albert Einstein College of Medicine). Succinimidyl-6-(biotinamido)-hexanoate (NHS-LC biotin) was acquired from Pierce (Rockford, IL). The steel block, ball bearing homogenizer was made by Auburn Tool and Die (Warwick, RI). Nitrocellulose membrane (0.45 µm) was purchased from BioRad Laboratories. Polyvinylidene fluoride (PVDF) membrane was obtained from Millipore. The enhanced chemiluminescence (ECL) kit, 2-Deoxy-D-[2,6-^{3}H] glucose (45 Ci/mmol), D-[U-^{14}C] glucose (310mCi/mmol), and L-^{35}S labeling mix (1000 Ci/mmol) were purchased from Amersham Life Science. All other reagents were of analytical grade from commercial sources.

Methods

Cell Culture and Glucose Deprivation

Endothelial cells, provided by Dr. Gary Visner (University of Florida), were originally isolated from 2 cm sections of human pulmonary artery obtained from heart transplant recipients. The tissue was placed in ice-cold saline for transport to the laboratory. The tissue was rinsed with sterile PBS (pH 7.5) to remove excess blood. The tissue was then incubated at 37°C for 15 min in 10 ml PBS containing collagenase (1mg/ml). The artery was laid flat and the endothelium gently scraped with a #10 scalpel blade to remove endothelial cells. The cells were dispersed in M199 medium containing antibiotics and 10% fetal bovine serum (FBS) and then spun in a centrifuge at 4°C at 800 x g for 10 min. The cell pellet was re-dispersed in M199 medium containing 20% FBS, glutamine (2mM), insulin (5 μg/ml), human transferrin (5 μg/ml), sodium selenite (5ng/ml), heparin (15 μg/ml), and bovine retinal derived growth factor (1 vial/200ml medium) and plated into a T-25 flask coated with 0.02% gelatin. The medium was changed every 2 days until the cells were just confluent. Once the cell line was established, the cells were maintained in M199 medium with 10% FBS, alone. The cells exhibited cobblestone morphology and endothelin-1 secretion until at least passage 25. For experiments, M199 medium was replaced with DMEM supplemented with 10% FBS.

Fibroblasts from patients with carbohydrate-deficient glycoprotein syndrome were provided by Dr. Jaak Jaeken (University Hospital, Gasthuisberg, Belgium). These cells, as well as normal human fibroblasts provided by Dr. Michael Kilberg, were grown in DMEM supplemented with 10% FBS until confluent.

3T3-L1 fibroblasts were cultured and differentiated as described by Frost and Lane (52). Cells were plated at approximately 3.5 x 10^4 cells/ml in DMEM supplemented with 10% calf serum with incubation conditions of 37°C and 7% CO_2 and fed once every two days with DMEM/10% calf serum until confluent. Two days post-confluency, cell monolayers were incubated for two days in DMEM containing 10% FBS, 0.5 mM methylisobutylxanthine, 0.25 μM dexamethasone, and 1 μg/ml insulin. Next, cells were incubated for two days in DMEM/10% FBS containing μg/ml insulin. Cells were then fed every two days with DMEM/10% FBS. Eight to twelve days post-induction, when cells were >95% differentiated, they were ready for use in experiments as adipocytes. For glucose-deprived adipocytes, the culture medium was replaced with glucose-free DMEM containing 10% dialyzed FBS supplemented with 25 mM fructose for the time period indicated.

Whole Cell Glucose Transport

The protocol for measuring glucose transport in 3T3-L1 adipocytes is as described previously (36;52). Cells in 35 mm plates were washed 3 times with 3 ml Krebs-Ringer phosphate buffer (KRP--128 mM NaCl, 4.7 mM KCl, 1.25 mM $CaCl_2$, 5.0 mM phosphate salts, pH 7.4). Plates were equilibrated in 950 μl of this buffer for 10 minutes at 37°C, followed by a 10 minute incubation after the addition of 50 μl of [^{3}H]2-deoxyglucose at a final concentration of 0.2 mM (1 μCi/μmol). To terminate the reaction, the plates were washed 3 times with 3 ml of PBS (120 mM NaCl, 2.7 mM KCl, 10 mM phosphate salts, pH 7.4). To quantitate radioactivity, the cells were lysed in 1.0 ml of 0.1% sodium dodecyl sulfate (SDS) and an aliquot was taken for measurement by scintillation counting.

For human cells, kinetic studies to determine Km, Vmax, and EC_{50} were performed. Glucose uptake was determined essentially as above. Deoxyglucose was added at the indicated concentrations for 10 minutes in the absence or presence of cytochalasin B. To prepare the various concentrations, [^{3}H]2-deoxyglucose was dried down under nitrogen and 0.2 M unlabeled deoxyglucose in KRP was added. This 0.2 M stock resulted in a 10 mM final concentration when 50 μl was added to 950 μl of buffer overlaying cells in a 35 mm plate. The specific activity remained constant at 650 cpm/nmol for all concentrations. A series of dilutions of this solution provided the stocks which gave 5, 2.5, 1, 0.5, 0.25, and 0.1 mM final concentrations per plate. Transport values at these concentrations were used to determine Km and Vmax from Lineweaver-Burk plots. To determine the EC_{50}, transport was also measured as with 3T3-L1 cells but incubations prior to the transport assay were in DMEM containing glucose with the indicated concentrations. This was accomplished by preparing glucose-free DMEM (0 mM) and mixing with appropriate volumes of 25 mM glucose. For the intermediate concentrations, a 10 mM stock of DMEM was prepared. From these, a series of dilutions provided concentrations ranging from 7.5 mM to 0.1 mM glucose-containing DMEM. To maintain the glucose concentrations over the 24 hour incubation, the medium was replaced every 4 hours at each concentration.

Subcellular Fractionation of 3T3-L1 Adipocytes

The 3T3-L1 adipocytes are difficult cells to reliably separate into subcellular fractions, as evidenced by the numerous variations of protocols in the literature. The procedure delineated here, developed by Fisher and Frost (53), accomplishes the subfractionation of these cells with substantial reproducibility. The technique, described by Weber et al. (54) for the fractionation of rat adipocytes, is adapted to the isolation of plasma membranes (PM), high-density 'microsomal' membranes (HDM), and low-density 'microsomal' membranes (LDM) from 3T3-L1 adipocytes (following the protocol for 5 to 8 rats). The major difference between the technique described here and the Weber protocol is the use of a steel block, ball-bearing homogenizer designed by Balch and Rothman (55). A tungsten ball-bearing with a diameter of 0.4990" provided a precise clearance of 0.0025". Five, 10 cm plates of 3T3-L1 adipocytes were glucose-fed or glucose-deprived for 12 hours. When pooled, these plates represented 60 million cells per condition. Cells were washed and incubated in KRP for 10 minutes then pooled by scraping into 4 ml/plate of TES buffer (20 mM Tris, pH 7.4, 1 mM EDTA, 255 mM sucrose) at 18°C. Cells from each treatment paradigm, in a total of 20 ml, was loadedinto a syringe attached to the pre-cooled steel block homogenizer, and passed through the chamber containing the ball-bearing to a second syringe 10 times at 4°C. A combination of differential and sucrose gradient centrifugation provided the means by which the three subcellular membrane fractions mentioned above were separated, as shown in Figure 2-1. Each membrane fraction was resuspended in 0.3 ml TES, frozen in liquid nitrogen, and stored at -20°C.

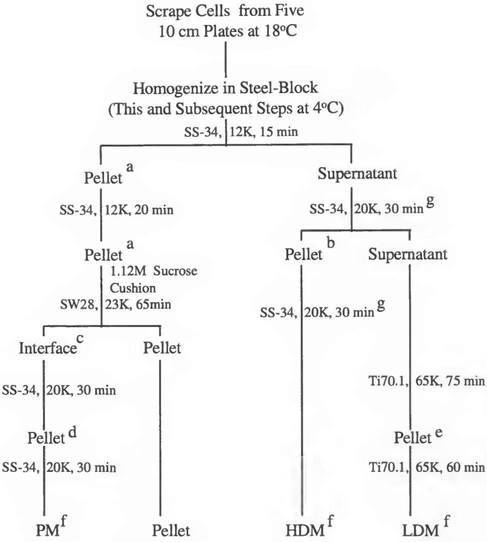

Figure 2-1 - Subfractionation of 3T3-L1 Adipocytes All pellets were resuspended by hand with 10 strokes (down/up = 1 stroke) using a Potter-Elvejhem type homogenizer. Volumes used for resuspension were the following: *a*, 20 ml TES; *b*, pooled multiple pellets into 10 ml TES; *c*, collect entire interface and bring to 10 ml with TES; *d*, 10 ml TES; *e*, pooled multiple pellets into 6 ml TES; *f*, 300 µl TES; *g*, used 15 ml Corex tubes--divided sample where necessary. RCF values at r_{max}: SS-34, 12K = 17,210 *x g*, 20K = 47,800 *x g*; SW28, 23K = 95,390 *x g*; Ti70.1, 65K = 388,000 *x g*.

Electron Microscopy

Images of membrane samples were made by the University of Florida Electron Microscopy Core using standard techniques. Briefly, samples were fixed in 2% glutaraldehyde buffered in PBS (pH 7.2) at room temperature for 1 hour, then washed with PBS twice. Post fixation was carried out in PBS-buffered 2% osmium tetroxide for 1 hour, followed by 3 washes with distilled water. A graded series of 15 minute ethanol washes (25%, 50%, 75%, 95%, 100%) was followed by two changes in 100% acetone as a transition solvent. Resin infiltration was performed in 1:1 Spurr's/ Epon mixture diluted with acetone at 30%, 50%, 70%, 100%, and 100% for 30 minutes per step. Polymerization took place at 60°C over two days. Samples were sectioned with a diamond knife on a Reichert Ultracut E and placed on 100 mesh formvar coated copper grids. Sections were post stained with 2% aqueous uranyl acetate and Reynold's lead citrate and viewed under a Hitachi H-7000 at 75 kV.

Markwell Assay for Protein Determination

All protein determinations were carried out using a modification (56) of the Lowry procedure (57). This assay uses the color-generating reaction of the Folin-Ciocalteu phenol reagent with the tyrosyl residues of protein in solution and compares the absorbance measurement of the sample to be determined against a standard curve. The standard curve was prepared in duplicate using a 1 mg/ml stock solution of bovine serum albumin to create a curve spanning from 0 to 100 µg. Each point on the curve was brought to a total volume of 100 µl with dH_2O. The buffer in which the unknown was measured was added to each standard, and 100 µl of dH_2O was added to each unknown so that volumes in all samples were equal. Then, 1 ml of a mixture of 100 parts solution 1 (2.0% Na_2CO_3, 0.4% NaOH, 0.16% NaKtartrate, 1.0% SDS) and 1 part solution 2 (4% $CuSO_4$) was added to each sample for a 10 minute incubation at room temperature. Folin and Ciocalteu's phenol reagent was added (0.1 ml, 1N), mixed, and samples incubated for 45 minutes. A spectrophotometer was then used to measure the absorbance of the samples in the visible part of the spectrum at a wavelength of 650 nm. The standard curve was plotted and a second order regression of the line was calculated with a computer program. The correlation coefficient value r^2 was always greater than 0.99. The unknown protein concentrations were calculated from the quadratic equation defining the standard curve.

Gel Electrophoresis

One-dimensional gel electrophoresis

One-dimensional SDS-polyacrylamide gel electrophoresis (SDS-PAGE) was performed essentially as described by Laemmli et al. (58). Protein samples were mixed with an equal volume of sample dilution buffer (4% SDS, 6M urea, 10% β-mercaptoethanol, 0.15 mg/ml bromophenol blue, 40% glycerol, and 20 mM Tris-base, pH 6.6). Gels were typically run at room temperature overnight at approximately 40V.

Two-dimensional gel electrophoresis

The advantage of two-dimensional (2D) over 1D SDS-PAGE is that proteins are separated not just by molecular weight, but in addition, by isoelectric point. A protein's isoelectric point is the pH at which its net charge is zero. At this pH, the protein is immobile in an electric field. In 2D gel electrophoresis, the first dimension allows isoelectric focusing (IEF) which makes use of a stable pH gradient to focus proteins by electrophoresis to their respective isoelectric points. This procedure was performed as previously described by Semple-Rowland et al. (59).

First dimension. Membranes in TES were diluted with an equal volume of IEF sample solution (6.4% NP-40, 6,5 mM DTT). For extractions, buffers contained NP-40 or other nonionic detergents. To remove insoluble material, extracts were clarified by centrifugation at (13,300 *x g*) for 5 minutes at 4°C in a microcentrifuge. Protein (up to 400 μg in 200 μl) was mixed with a 4% acrylamide solution containing 9M urea, 2% NP-40, and 2% carrier ampholytes (pH 3.5 to 10). To initiate polymerization, 2 μl TEMED (N,N,N',N'-tetramethylethylenediamine) and 2 μl APS (ammonium persulfate) were added. Gels were cast 11 cm long in 3 mm diameter glass tubes. The anodic and cathodic buffers were 10 mM phosphoric acid and 20 mM sodium hydroxide, respectively. Gels were run at 350V for 18 hours followed by 800V for 2.5 hours. The gels were then extruded using a water-filled syringe fitted with tubing to envelop the glass tube and incubated in equilibration buffer (62.5 mM Tris-HCl, pH 6.8, 5% β-mercaptoethanol, 2.3% SDS, 10% glycerol) for 30 minutes. The pH gradient was determined by running an identical gel with 200 μl TES:IEF sample solution in place of protein, cutting it into 0.5 cm pieces, soaking each piece in 1 ml distilled water for at least 2 hours, and measuring each pH.

Second dimension. One SDS-PAGE gel was poured for each tube gel, which was layered onto the stacking gel using embedding agarose (1% agarose in SDS-PAGE stacking gel buffer). Molecular weight standards were prepared by mixing 10 µl of low molecular weight standards (BioRad) with 300 µl 1% agarose in equilibration buffer and allowing it to solidify in a tube, which was cut and placed beside the sample gel. The marker gel and sample gel were then overlaid with more embedding solution which contained bromophenol blue to allow the gel to be tracked while running. The second dimension was run overnight as described above for one-dimensional gel electrophoresis.

Electrotransfer and Immunoblotting

For immunoblotting, or western analysis, protein samples were electrotransferred from the SDS-PAGE gel to a nitrocellulose membrane which had been previously soaked for 30 minutes in transfer buffer (25 mM Tris-base, 192 mM glycine, 20% methanol). The proteins were transferred at 250 mA for 2 to 2.5 hours at 4°C (60) or overnight at 30V. To visualize proteins after transfer, the nitrocellulose was stained with amido black (0.2% in 40% methanol, 10% acetic acid), destained (40% methanol, 10% acetic acid), and washed in distilled water. The blot was then blocked to inhibit nonspecific antibody interactions in Tris-buffered saline (20 mM Tris, 137 mM NaCl)/0.1% Tween-20 (TBS-T) containing 5% non-fat dry milk (NFDM) for 1 hour at room temperature with agitation on an orbital shaker. A washing step followed which consisted of 3 washes in TBS-T for 1 minute each and 2 more washes for 5 minutes each. The primary antibody was then applied to the blot for 1 hour in TBS-T/ 5% NFDM with agitation. After this, the blot was washed as described above. Following this, the blot was incubated with the secondary antibody, an anti-IgG linked to horseradish peroxidase (HRP), for 1 hour in TBS-T/ 5% NFDM with agitation. The final washes in TBS-T, 4 for 1 minute each and 3 for 5 minutes each, were to ensure that no unreacted IgG-HRP remained. The ECL detection method was used according to manufacturer's directions, followed by exposure to Amersham Hyperfilm. Subsequent densitometry was performed on a Visage Bioscan video densitometer in the linear range of the film and the luminescent assay.

RNA Isolation and Northern Analysis

RNA isolation and northern blotting was performed as previously described (36). Briefly, a 20 µg sample of RNA was loaded onto a 1% formaldehyde-agarose gel which was run overnight with buffer recirculation. After washing the gel, the RNA was electrophoretically transferred to an uncharged nylon membrane (Hybond, Amersham) and cross-linked with ultraviolet light for 3.5 minutes. To make the GLUT1 probe, 0.5 μg of the cDNA was boiled for 5 minutes and cooled for 3 minutes followed by incubation with primers, $[^{32}P]$dATP, unlabeled deoxynucleotides, and DNA polymerase. The labeled DNA was separated from free nucleotides by gel chromatography using Sephadex G50 and used to probe the RNA electrotransfer. This hybridization step was carried out overnight (~15 hours) in a buffer containing 1% BSA (radioimmunoassay grade), 1 mM EDTA, 0.5 M Na_2HPO_4, pH 7.2, and 1% SDS at 65°C. The nylon membrane was washed 3 x 20 minutes under high stringency in 1 mM EDTA, 0.5 M Na_2HPO_4, pH 7.2, and 1% SDS at 65°C and exposed to film at -70°C.

Plasma Membrane Vesicle Transport

Transport of glucose in plasma membrane vesicles was performed as previously described (53). Plasma membranes were prepared from glucose-fed and glucose-deprived cells using the subfractionation protocol described above. Samples were brought to 1 mg/ml in TES and resuspended 10 times with a 27-gauge needle. In each experiment, 20 μg of membrane protein were incubated in the absence or presence of 20 μM cytochalasin B for 10 minutes at room temperature. Each sample was then pulsed with 20 μl of 0.1 mM D-glucose in TES containing 1 μCi of D-$[^{14}C]$glucose for 15 seconds, although the uptake was linear for at least 30 seconds. Transport was stopped by adding 1 ml of ice-cold stop solution (0.3 mM phloretin, 0.1 mM D-glucose, 10 μM cytochalasin B in TES). This solution was filtered through a 0.22 μm filter (Millipore) on a single port vacuum apparatus (Fisher). Filters were rinsed 3 times with 3 ml of stop solution and placed in 1 ml of 0.1% SDS for 30 minutes. Scintillant (10 ml) was then added for counting.

Cell Surface Biotinylation

Cell surface membrane proteins were tagged and detected by making use of biotin, its reactivity with streptavidin, and the ECL detection method. Biotin, a small molecule of 244 daltons, can react with available functional groups on proteins. Several reagents are available for the biotinylation of different functional groups. The reagents used here were chosen, based on manufacturer's recommendations, so that cell surface membranes would be recognized with maximum efficiency. To that end, the biotinylation reagent selected was NHS-LC Biotin, an N-hydroxysulfosuccinimide (sulfo-NHS) ester of biotin with a long chain (LC) spacer arm of 22.4 angstroms in length. The sulfonate group confers water solubility, on the NHS ester of biotin, as well as the additional characteristic of membrane impermeability. These features allow the incubation of intact cells in buffer containing the reagent, which exposes only surface proteins to biotinylation. NHS esters react with primary amines, available on exposed N-termini and lysine residues. In the reaction, Sulfo-NHS leaves as an amide bond forms between the protein and ester. The inclusion of an extended spacer arm, as with NHS-LC biotin, optimizes the reactivity of biotin with streptavidin. Streptavidin is a tetrameric protein with identical 60 kDa subunits, each capable of binding one biotin molecule. Each subunit is large and the binding site for biotin is buried 9 angstroms beneath the surface of streptavidin. Thus, the long chain spacer enhances reactivity by reducing steric hindrance. With a K_a of 10^{15} M^{-1}, the biotin-avidin/streptavidin bond is the strongest noncovalent biological interaction known between protein and ligand. Streptavidin-HRP was subsequently used to label biotinylated cell surface proteins, to allow detection by ECL.

Glucose-fed or glucose-deprived cells, adherent to 10 cm plates, were washed 3 times with PBS (pH 8.2) containing 1mM $CaCl_2$ and 1 mM $MgCl_2$ (PBSCM) at 4°C and allowed to equilibrate in 4 ml for 10 minutes. The deprotonated form of the primary amine, with which the NHS ester reacts, is available above neutral pH, but hydrolysis of the ester becomes increasingly favorable at higher pH. Therefore, the choice of pH 8.2 was to optimize reaction conditions. Buffer was aspirated and cells were then overlaid with 2.5 ml of PBSCM containing 875 μg of NHS-LC biotin. After 1 h, cells were washed twice with PBSCM and overlaid with 4 ml of TES for 10 minutes to quench unreacted NHS-LC biotin, as the Tris in TES contains amines which compete with those on cell surface proteins for the reaction.

Cells were either subfractionated as described above or extracted. Proteins from membrane fractions were separated by SDS-PAGE and electrotransferred. Biotinylated proteins were detected using streptavidin-HRP and ECL. Total membranes were collected for extraction by scraping each 10 cm plate of cells in 4 ml of TES, sonicating for 30 seconds using a Branson Sonifier 450 at power setting #2, 50% duty cycle, and spinning in a Ti 70.1 rotor at 212,000 *x g* for 70 minutes. Pellets were extracted in 1 ml extraction buffer, containing 1 mM EDTA, 2% $C_{12}E_9$, and 0.1% SDS. Insoluble material was removed by centrifugation for 5 min at 13,300 *x g*. Clarified extract was separated and rotated end-over-end with 50 μl of a 50% slurry of streptavidin agarose for 6 hours. The beads were collected by centrifugation with a brief pulse in a microcentrifuge and washed several times with extraction buffer. After washing, extraction buffer was aspirated and 100 µl of sample dilution buffer was added to the beads and incubated for 30 minutes at 37°C. The released proteins were separated by SDS-PAGE and transferred to nitrocellulose. For detection with streptavidin-HRP and ECL, the procedure was similar to that described for immunoblotting. Instead of the primary and secondary antibody steps, after the initial blocking and washing of the blot, streptavidin-HRP was applied at a 1:50,000 dilution in TBS-T/ 0.5% NFDM for 1 hour. The nitrocellulose was then washed as in the immunoblotting procedure and the ECL detection method applied.

Isolation of GLUT1-Containing Vesicles

GLUT1-enriched vesicles from PM, HDM, and LDM fractions were isolated using magnetic beads conjugated to anti-GLUT1 as previously described (61). Tosyl-activated magnetic beads, 4.5 µm in diameter (M-450 Dynabeads, Dynal), were covalently bound with goat anti-rabbit IgG according to the manufacturer's directions. The IgG was added at a concentration of 5 µg per 10^7 beads. Efficiency of binding was 43% which was within the expected range. In a microcentrifuge tube, 1 mg of beads was blocked in 1 ml blocking buffer (100 mM K_3PO_4, 0.5% BSA, pH 7.4) overnight at 4°C with end-over-end rotation. Blocked beads were separated with a magnetic particle concentrator (MPC) and then incubated in 1 ml blocking buffer with or without 10 μg peptide-purified anti-GLUT1 IgG overnight at 4°C with rotation. Beads were then washed 3 times for 20 minutes each in blocking buffer. Membranes vesicles were isolated from 3T3-L1 adipocytes using the subfractionation procedure described earlier in this chapter. The membranes were passed 20 times through a 27-gauge needle to achieve uniform size of vesicles. Fifty micrograms was added to the beads in a total volume of 1 ml for incubation overnight at 4°C with rotation.

Beads were separated from the supernatants with the MPC. Supernatants, which contain membrane vesicles that were not adsorbed by the beads, were diluted with 3 ml of wash buffer (100 mM K_3PO_4, pH 7.4) in order to reduce the amount of BSA. Nonadsorbed membrane vesicles were collected at 212,000 *x g* for 1 hour. The beads were exposed to three washes for 20 minutes and collected each time with the MPC. Membrane proteins were eluted with 100 μl Laemmli sample dilution buffer containing 6 M urea and 10% β-mercaptoethanol at 37°C for 30 minutes. Nonadsorbed membrane vesicles were resuspended in 100 μl of the above sample buffer. Adsorbed and nonadsorbed membrane proteins from control versus anti-GLUT1-conjugated beads were resolved on 10% SDS-PAGE. The proteins were transferred to nitrocellulose for immunoblot analysis.

Metabolic Radiolabeling of 3T3-L1 Adipocytes

Newly synthesized proteins were visualized by metabolically labeling cells with the radioactive amino acids, ^{35}S methionine and ^{35}S cysteine. Cells in 10 cm plates were first incubated for 1 hour in 8 ml of depletion medium (glucose-free DMEM containing no methionine or cysteine, supplemented with either 25 mM glucose for control or 25 mM fructose for glucose-deprived cells). This lowers the concentration of intracellular pools of cysteine and methionine. Depletion medium was replaced with labeling medium, which consisted of 2 ml/plate of depletion medium containing 200 μCi/ml ^{35}S labeling mix. After 3 hours, cells were harvested and fractionated either for total membranes or subcellular membrane fractions. Proteins in the fraction of interest were separated by gel electrophoresis. Gels were fixed in 10% TCA/40% methanol for 30 minutes, rinsed in water for 30 minutes, soaked in 1 M sodium salicylate for 1 hour, and then dried at 60°C under vacuum. Once dry, the gels were exposed to film and cooled to -70°C for a period of time related to the counts per minute (cpm) of radioactivity loaded. When the order of magnitude was 10^7 cpm, the exposure time was several hours, while 10^6 cpm was from 1-2 days, and 10^5 cpm was several days. Before development, the film was brought to room temperature.

Preparation of Protein for Microsequencing

Concentration of glucose-dependent protein

Sequence information was desired for a protein "spot" on two-dimensional gel electrophoresis which was enriched in samples from glucose-deprived cells versus controls. This spot shall be referred to as GDP, for glucose-dependent protein. GDP was visible when gels were stained with Coomassie Blue (50% ethanol, 10% acetic acid, 2.5 mg/ml Coomassie Blue) and destained (20% ethanol, 10% acetic acid). A minimum of 50 to 100 pmol of material was required for internal sequencing. To generate this amount of GDP, 40 isoelectric focusing gels were run from which GDP was isolated and concentrated using the procedure described below (illustrated in Figure 2-2). Each IEF gel was loaded with 750 μg to 800 μg of protein from total membrane preparations. The tube gels were extruded and the acidic ends of each were placed side-by-side on the second

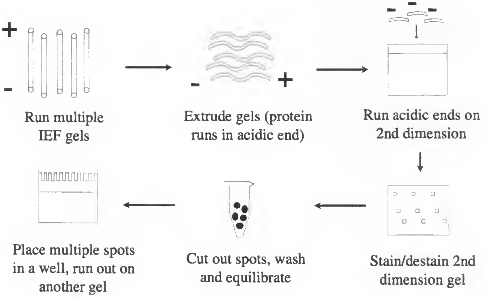
+
-
Run multiple IEF gels
-
+
Extrude gels (protein runs in acidic end)
Run acidic ends on 2nd dimension
Stain/destain 2nd dimension gel
Cut out spots, wash and equilibrate
Place multiple spots in a well, run out on another gel

Figure 2-2 - Isolation and Concentration of Glucose-dependent Protein Protein from the acidic (~pH 4.5 to 6) region of 40 isoelectric focusing gels was run on second dimension SDS-PAGE. The spots representing the GDP were visualized by staining, excised, and prepared for a subsequent SDS-PAGE run. In this manner, 8 spots per well were concentrated to 5 bands of approximately 50 pmol.

dimension. These gels were stained with Coomassie as described above and the GDP spots were excised. Gel slices were stored in Coomassie destain solution at 4°C until all were ready for concentration. When 40 slices were obtained, all were washed 4 times for 15 minutes each with dH_2O to remove destain followed by equilibration in sample dilution buffer for 15 minutes at room temperature. The slices, which constituted greater than 50 pmol of protein, were concentrated into 5 bands by running 8 per well on 1-D 10% SDS-PAGE. The purpose for concentrating the 40 gel slices into 5 bands was to reduce the gel volume containing the protein in order to maximize efficiency of the in-gel digest necessary for internal sequencing.

Microsequencing of glucose-dependent protein

In situ enzymatic cleavage of GDP, concentrated as described above, was performed by the University of Florida Protein Chemistry Core using endoproteinase Lys-C, which cleaves at the C-terminal side of lysine residues. This enzyme was chosen instead of trypsin, which cleaves polypeptides at both lysine and arginine residues, because of the greater likelihood of longer peptide fragments. Briefly, gel slices were washed 3 times in a volume small enough to cover them with 0.2 M ammonium bicarbonate (AB)/ 50% acetonitrile at 30°C. Gel slices were dried in a rotary evaporator, rehydrated with 0.2 M AB (in 5 µl volumes) while adding endoLys-C (0.5 mg in 0.5 µl) until gels were covered, and incubated overnight at 30°C. The reaction was stopped with 10% trifluoroacetic acid (TFA). The supernatant was saved as extract, pooled with those from 3 incubations of gels in 100 µl of 0.1% TFA/ 60% acetonitrile. Extract volume was reduced to approximately one third, from which peptides were isolated. A small-bore Hewlett-Packard 1090 model HPLC instrument with a reverse-phase C18 column was used to separate peptide fragments. Fractions were analyzed with a mass spectrometer. Sequence data was obtained with an Applied Biosystems Model 473A Gas Phase Protein Sequenator with an online PTH (phenylthiohydantoin) analyzer.

Detergent Extraction of Proteins

To separate proteins on the basis of detergent solubility, 3T3-L1 adipocytes in 10 cm plates were extracted in 0.5% NP40 in PBS (pH 7.4). Cells, treated as described in the text, were first rinsed with and incubated in KRP at 37°C for 10 minutes. Then cells were exposed on ice to 4 ml per plate of the above detergent solution in the presence of proteinase inhibitors (20 µg/ml each of aprotinin, leupeptin, pepstatin, N-tosyl-L-phenylalanine chloromethyl ketone, N-tosyl-L-lysine chloromethyl ketone, and 1 mM phenylmethyl sulfonyl fluoride) for 10 minutes. The NP40 soluble proteins were decanted from each plate. The NP40 insoluble proteins remained on the plate and were resuspended in 1 ml of the detergent solution containing proteinase inhibitors. Aliquots were stored for protein analysis and/or scintillation counting. Proteins were separated by one- or two-dimensional gel electrophoresis and visualized using immunoblotting or autoradiography.

CHAPTER 3

EFFECT OF GLUCOSE DEPRIVATION ON GLUCOSE TRANSPORT AND TRANSPORTER DISTRIBUTION IN 3T3-L1 ADIPOCYTES

Introduction

The 3T3-L1 cell line has provided an important tool in the study of glucose transport because this adipocyte model system allows the investigation of chronic treatment paradigms. This has been a distinct advantage in examining the effects of glucose deprivation which increases the rate of glucose transport in a time- and protein synthesis-dependent manner (31-33). This contrasts with the acute effect of insulin (52). Although the deprivation phenomenon has been documented in numerous cell types, it is evident that cell type-specific mechanism(s) define the increase in transport activity, as reviewed previously (21). In chick embryo fibroblasts (34), glia (35), myocytes (27), and L6 muscle cells (62), an increase in GLUT1 mRNA has been demonstrated, resulting in greater levels of GLUT1 protein for insertion into the plasma membrane. This latter aspect, however, has not been tested. In murine fibroblasts

(24;63), GLUT1 increases not as a function of increased message availability but via a block in GLUT1 degradation. A new equilibrium presumably is established between GLUT1 stored inside the cell versus that expressed on the cell surface. As shown by Kitzman et al. (36), the level of GLUT1 in 3T3-L1 adipocytes does not change during the time in which transport activity increases(36), confirming the earlier work of Reed et al. (32). With extended deprivation, the level of GLUT1 does increase but as a function of the accumulation of an aberrant form of GLUT1 (36). Importantly, the appearance of the lower molecular weight glycoform of GLUT1 does not correlate with further changes in transport activity. A second consideration in 3T3-L1 adipocytes is the contribution to transport activity by GLUT4, the insulin-responsive glucose transporter. While the levels of GLUT4 mRNA fall during glucose deprivation (33;36), it has been reported that GLUT4 protein expression is unchanged (33). From these observations, two mechanisms might underlie the deprivation-induced increase in transport activity: translocation of either GLUT1 or GLUT4 from intracellular storage compartments or activation of pre-existing cell surface transporters. The goal of this section is the examination of the role, if any, of translocation in glucose-deprived 3T3-L1 adipocytes.

Results

Effect of Glucose Deprivation on Uptake of [^{3}H]2-deoxyglucose

Glucose deprivation increases the rate of glucose transport in 3T3-L1 adipocytes (31-33;36). Those data were confirmed here with the measurement of glucose transport in intact 3T3-L1 adipocytes. Figure 3-1 demonstrates a 10-fold increase in transport activity in cells deprived of glucose for 12 hours relative to controls. Total glucose deprivation was implemented to maximize the activation phenomenon. However, Figure 3-1 also illustrates that fructose, which provides osmotic balance with controls as well as substrate for intermediary metabolism and protein glycosylation in the absence of glucose, interfered little with transport activation. For this reason, glucose deprivation was carried out in the presence of 25 mM fructose throughout the remainder of experiments.

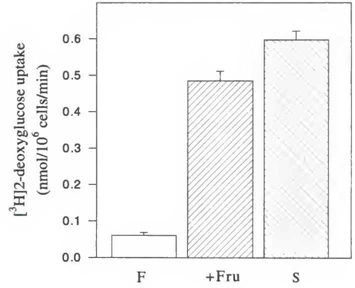

Figure 3-1 - Effect of Glucose Deprivation on Uptake of $[^3H]$2-deoxyglucose 3T3-L1 adipocytes in 35 mm plates were incubated for 12 hours in medium in the absence *(S)* or presence *(F)* of 25 mM glucose, or with 25 mM fructose in a glucose-free environment *(+Fru)*. Transport of deoxyglucose was assayed for 10 min. The rates, reported as nmol/10^6 cells/min + S.E., are for duplicate assays and are representative of two independent experiments.

Subcellular Fractionation in 3T3-L1 Adipocytes

The goal of this set of experiments was to determine what part translocation plays in the response of 3T3-L1 adipocytes to glucose deprivation. Therefore, we first required a dependable method for subfractionation of these cells. This was accomplished using a steel-block, ball-bearing homogenizer designed by Balch and Rothman (55) for the purification of endosomes, in combination with a detailed subfractionation procedure reported by Weber et al. (54) for isolated rat adipocytes. The protocol is delineated in Materials and Methods. The choice of homogenization clearance affects protein recovery (54) and the use of a steel block homogenizer allowed this parameter to be manipulated. This is illustrated in Figure 3-2, which demonstrates the reason for using a clearance of 0.0025". The 0.4990" ball-bearing that provided this clearance gave the best results for location of the transporters. Specifically, there was more GLUT1 in all three fractions resulting from 0.4990" clearance. Also, GLUT4 had greater recovery in the intracellular membrane fractions. Reliability was established by demonstration of both reproducibility and accuracy of the procedure. Protein recovery in the initial homogenates and subcellular fractions from the control and glucose-deprived cells was

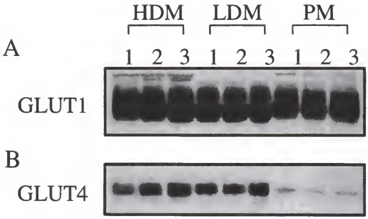

Figure 3-2 - Effect of Clearance Size on Subfractionation Glucose-fed 3T3-L1 adipocytes were subfractionated, with different sized ball-bearings in the chamber of the steel-block homogenizer. Lanes marked *1* represent fractions isolated with a 0.4955" (0.0060" clearance) ball-bearing. In lanes *2* and *3*, 0.4980" (0.0035" clearance) and 0.4990" (0.0025" clearance) ball-bearings were used, respectively. Each lane represents 70 µg of protein. *Panel A*, GLUT1 and *Panel B*, GLUT4 were analyzed by immunoblotting with specific antibodies using enhanced chemiluminescence.

similar over many experiments, indicating reproducibility (see Table 3-1). Including the mitochondrial/nuclear fraction, membrane constituted 35% of the recovered protein.

To verify the efficiency of the fractionation procedure, two approaches were utilized. First, the distribution of plasma membranes was followed by biotinylating cell surface proteins prior to subfractionation. Second, the appearance of certain proteins selected for their presence in PM or intracellular membranes was examined. Biotinylated proteins were enriched in the PM fraction over the HDM and LDM (Figure 3-3). A dot blot analysis of equal protein (50 ng) from each fraction was used to quantitate this enrichment (data not shown). Relative to homogenate, the PM fraction was enriched in biotinylated proteins by 12-fold. Based on the total recovery of protein in each fraction, less than 2%

Table 3-1 - Protein Recovery from Subcellular Fractionation

Fraction	Glucose-fed	Glucose-deprived
Homogenate	33.2 ± 2.9	31.0 ± 3.0
PM	0.42 ± 0.05	0.41 ± 0.06
HDM	0.66 ± 0.08	0.64 ± 0.09
LDM	1.22 ± 0.25	1.34 ± 0.14

3T3-L1 adipocytes were glucose-fed or glucose-deprived for 12 hours prior to subfractionation. The total amount of protein for homogenates and membrane fractions was determined from four independent experiments and is reported as mg ± S.E.

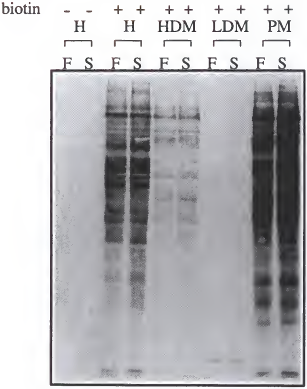

Figure 3-3 - Distribution of Cell-surface Biotinylated Proteins Cells were incubated for 12 hours in medium in the presence of 25 mM fructose in a glucose-free background *(S)* or 25 mM glucose *(F)*. After biotinylation, cells were subfractionated. Each lane represents 25 µg of protein. Samples of homogenate *(H)* from non-biotinylated (-) and biotinylated (+) cells were loaded as controls for comparison to HDM, LDM, and PM. Biotinylated proteins were detected with streptavidin-horseradish peroxidase using enhanced chemiluminescence. This figure is representative of two independent experiments.

of biotinylated proteins comigrated with the LDM fraction, while approximately 10% of biotinylated proteins comigrated with the HDM fraction. Confirmation that 10% of the PM proteins migrated with the HDM fraction was achieved by densitometric analysis of immunoblots performed using an antibody against the α-subunit of Na^+,K^+-ATPase, which gave identical results (Figure 3-4). To analyze contamination of the PM fraction with membranes of intracellular origin, the relative amounts of GRP78, an endoplasmic reticulum chaperone, sialytransferase, a trans-Golgi marker, and GLUT4, an endosomal marker (64) were measured in membrane fractions using antibodies specific for each protein. GRP78 was localized predominantly to the HDM fraction, with about 12% cross-over to the PM (Figure 3-4). Sialyltransferase was also localized to the HDM fraction with less than 2% comigrating with the PM fraction (data not shown). Only 3% of GLUT4 colocalized with the PM fraction in the presence or absence of glucose (Figure 3-4, Table 3-2), demonstrating that the PM is relatively free from endosomal contamination.

After verifying that they contained the appropriate membranes, the fractions were further characterized. First, images were obtained of each fraction by electron microscopy. The electron micrographs shown in Figure 3-5 illustrate that the membranes form vesicles when isolated.

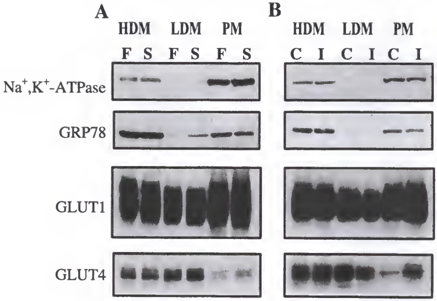

Figure 3-4 - Subcellular Distribution of GLUT1 and GLUT4 *Panel A*, membrane fractions were prepared from cells incubated for 12 hours in medium in the presence of 25 mM fructose in a glucose-free background *(S)* or 25 mM glucose *(F)*. *Panel B*, a second experiment was performed on glucose-fed cells treated in the absence © or presence *(I)* of 1 μM insulin. HDM, LDM and PM fractions were loaded, 70 μg per lane. GLUT1, GLUT4, GRP78, and Na$^+$,K$^+$-ATPase were analyzed as appropriate by immunoblotting with specific antibodies using enhanced chemiluminescence. Subsequent densitometry was performed in the linear range of the film and the luminescent assay.

Table 3-2 - Subcellular Distribution of GLUT1 and GLUT4

Transporter	Condition	HDM	LDM	PM
GLUT1	C	38.9 ± 2.6	40.7 ± 4.5	20.4 ± 2.3
	S	37.0 ± 0.2	45.1 ± 0.3	17.9 ± 0.1
	I	42.4 + 1.4	26.0 ± 2.8	31.6 ± 2.7
GLUT4	C	31.8 + 3.3	65.5 ± 3.8	2.6 ± 0.7
	S	29.2 ± 0.7	67.9 ± 3.2	2.9 ± 2.5
	I	45.8 ± 3.8	32.2 ± 5.6	22.0 ± 5.6

Membrane fractions were prepared and densitometry performed as described in the legend for Figure 3-3. The distribution of each transporter is based on protein recovered in each fraction. The amount of transporter present in each fraction is reported as the average percentage ± S.E., with 100% representing the total of the three fractions. For results from control cells (C), *n* = 5; for glucose-deprived cells (S), *n* = 2; and for insulin-treated cells (I), *n* = 3.

Analysis of the micrographs indicates that the average diameter of the vesicles in the PM and HDM fractions is approximately 0.5 μm. Also evident is the granular appearance of the LDM fraction. Even under high magnification, the LDM structures appear too small to effectively estimate their size. Second, the magnetic bead technique which was developed to isolate GLUT1-containing vesicles from subcellular fractions (see Materials and Methods) was used to illustrate the relative orientation of the vesicles in each fraction. In Figure 3-6, lanes 1, 5, and 9 (- anti-GLUT1) serve as controls, indicating the nonspecific interaction of proteins from the PM, HDM, and

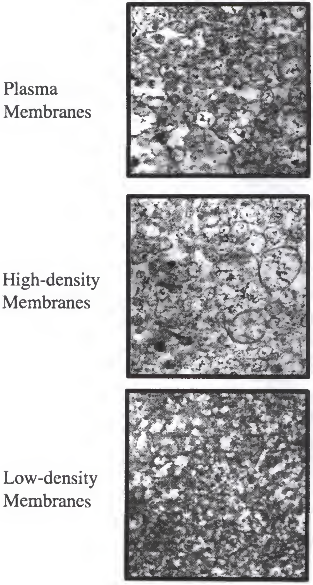

Figure 3-5 - Electron Micrographs of Membrane Fractions
Microscopy was performed as described in Materials and Methods.

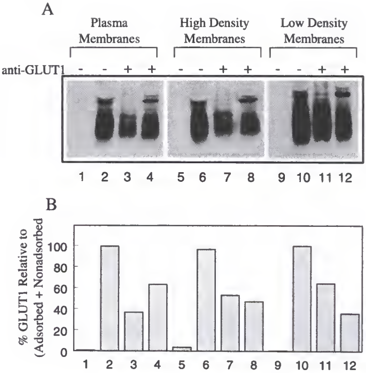

Figure 3-6 - Orientation of Vesicles from Subcellular Fractions *Panel A*, anti-GLUT1 immunoblot, visualized by enhanced chemiluminescence (ECL). Membrane samples were isolated and incubated with magnetic beads coated with nonspecific antibody alone (-) or with anti-GLUT1 IgG (+) as described in Materials and Methods. Odd lanes, membrane vesicles adsorbed by beads; even lanes, nonadsorbed membrane vesicles. *Panel B*, densitometric analysis of *Panel A* performed in the linear range of the film and the ECL reaction, with corresponding lanes numbered as in *Panel A*. This experiment is representative of three independent experiments.

LDM fractions with magnetic beads conjugated to only goat anti-rabbit IgG. These lanes are blank, which demonstrates that the non-specific antibody does not interact with GLUT1-containing vesicles. In contrast, lanes 3, 7, and 11 show the amount of GLUT1 in vesicles bound to beads coated with anti-GLUT1 (+ anti-GLUT1). For each of the four membrane groups, the first lane represents interactions with non-specific antibody. In the second lane are the membranes which are not bound to the non-specific antibody, that is, the entire sample. The third lane contains the membrane proteins collected with anti-GLUT1, as mentioned, and the fourth lane represents the membrane proteins from vesicles that remain in suspension. Densitometric analysis of lanes 3 and 4 reveals that, from plasma membranes, 37% of GLUT1 was collected with the anti-GLUT1-coated magnetic beads. This result means that the cytoplasmic sides of these vesicles face outward and thus have an inside-out orientation (Figure 3-6B). The membranes that did not bind to the beads (lane 4) likely have an opposite orientation as the maximum binding capacity of the beads was not achieved. The needle resuspension (or revesiculation) step is likely to allow reorientation of the vesicles. The intracellular vesicles contain a greater proportion of vesicles with the cytoplasmic face exposed (HDM, 53%; LDM, 65%) which is expected as this is their normal orientation in intact cells. Combined, these experiments demonstrate that the above methodology for the subfractionation of 3T3-L1 adipocytes is effective and reproducible.

Distribution of GLUT1 and GLUT4

The subfractionation technique described above was employed to examine the subcellular distribution of the two glucose transporters present in 3T3-L1 adipocytes, GLUT1 and GLUT4. The response of transporters to glucose deprivation was measured by immunoblotting with antibodies specific for each transporter (Figure 3-4A). GLUT4, as discussed above, is an endosomal marker protein (64). As expected, GLUT4 comigrates with the intracellular membranes and is enriched in the LDM fraction (Figure 3-4A). The distribution of transporters based on protein in each fraction was determined, and is shown in Table 3-2. To reiterate, only 3% of GLUT4 was localized in the PM fraction, suggesting that GLUT4 contributes little to basal transport and that it does not underlie the mechanism of transport activation. The distribution of GLUT1 in membrane fractions isolated from glucose-fed and glucose-deprived cells was examined next. Densitometric analysis of GLUT1, including the mitochondrial/nuclear fraction, revealed 70% recovery of

GLUT1 relative to the homogenate. Figure 3-4 shows GLUT1 distribution among the HDM, LDM and PM fractions only, as these fractions contain 12-19 times more GLUT1 than the mitochondrial/nuclear fraction. Based on protein recovered in each of these fractions, 20% of GLUT1 was calculated to reside on the cell surface (Table 3-2). To provide a positive control for translocation, an experiment was included in which glucose-fed cells were acutely stimulated with insulin (Figure 3-4B). With a 10 minute exposure to 1 μM insulin, the decrease in GLUT1 in the intracellular fractions (40%) corresponded to a nearly equal increase in the PM. GLUT4 content was reduced in the LDM by about 50%. The densitometric value for the loss in the LDM fraction was nearly equal to that which translocated to the PM. Thus, the control shows the capacity of the subfractionation technique to detect translocation events. Importantly, Figure 3-4A shows that glucose deprivation did not alter the localization of GLUT1.

Plasma Membrane Vesicle Transport

The plasma membrane is the site of glucose transport. However, the preceding experiments show that GLUT1, the major transporter present at the cell surface, does not change levels in response to glucose deprivation.

Therefore, it was of interest to determine whether PM vesicles isolated from glucose-deprived cells retain elevated transport activity. Figure 3-7 shows the comparison of vesicle transport data derived from glucose-deprived PM versus glucose-fed PM, using cytochalasin B to correct for nonspecific transport. No difference in transport activity between glucose-fed and glucose-deprived vesicles was seen in the presence of cytochalasin B, suggesting that vesicle volume does not change. The results indicate that transport in glucose-fed PM vesicles was below the limit of detection. However, transport in glucose-deprived PM vesicles was consistently observed as a significant increase over background. These results led to the investigation of plasma membrane proteins in glucose-fed versus glucose-deprived cells.

Conclusions

The results in this chapter first establish that the subfractionation protocol described reproducibly yields good separation of intracellular membranes. This conclusion was reached using two separate techniques to determine the distribution of membranes--cell surface biotinylation and immunoblotting with antibodies to specific marker membrane

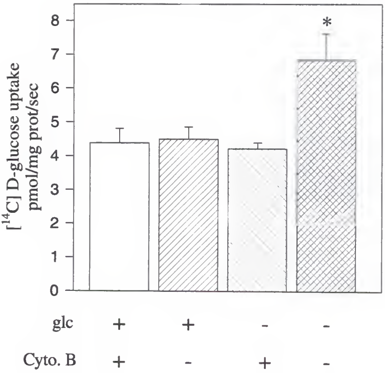

Figure 3-7 - Effect of Glucose-deprivation on Glucose Uptake in Plasma Membrane Vesicles Plasma membrane vesicles were isolated from glucose-deprived *(-glc)* and glucose-fed *(+glc)* cells. Uptake of D[^{14}C]glucose was measured in the presence and absence of cytochalasin B *(Cyto. B)* using a filtration assay. The rates are reported as pmol/mg protein/s + S.E., n = 20: *,, p = 0.002 for glucose-deprived minus versus plus cytochalasin B.

proteins. The extent of membrane purification was similar to that described by Weber et al. (54) for isolated rat adipocytes (54). With our fractionation procedure, we have shown that GLUT1 is the major transporter in the PM in both glucose-fed and glucose-deprived 3T3-L1 cells. Table 3-2 shows that 20% of the GLUT1 pool resides on the cell surface, corroborating cell surface photolabeling data (65;65). Glucose deprivation does not change GLUT1 localization. Concerned that our protocol would not detect movement of transporters, we verified the ability of insulin to stimulate the recruitment of GLUT4 as a means to detect a translocation event. Our observations were similar to previously published data on the insulin-induced translocation of the glucose transporters in 3T3-L1 adipocytes (37;66). Therefore, translocation of GLUT1 from intracellular membranes to the PM does not appear to be responsible for elevated transport activity in response to glucose deprivation. Even if the entire pool of GLUT1 translocated to the PM with glucose deprivation, we would predict only a 5-fold change in transport activity while a 10-fold change is actually observed. However, results in this section demonstrate that glucose deprivation does not change GLUT1 localization. Finally, we showed that PM vesicles isolated from glucose-deprived cells exhibit elevated transport activity.

The mechanisms behind the deprivation phenomenon are cell-type specific, as mentioned in Chapter 1,. Van Putten and Krans (31) observed a change in V_{max} and not K_m in glucose-deprived 3T3-L1 adipocytes. Possible explanations for increased transport under these circumstances include greater numbers of transporters or increased activity of the available transporters. In contrast, we have observed in a previously unstudied cell type an example of transport activation which takes place presumably via a more complex mechanism. Human pulmonary aortic endothelial cells (HPAEs), when glucose-deprived, exhibit a 4- to 5-fold enhancement in glucose transport. Both Vmax and Km change with glucose deprivation in HPAE cells. Also, transport activation appears to be dependent on both RNA and protein synthesis (see Appendix). The mechanism in 3T3-L1 adipocytes elicits no change in transporter affinity and requires new protein synthesis. Building on earlier work, our subfractionation protocol has verified that GLUT1 levels do not change and has shown that the transporters are not translocated to the cell surface in response to glucose deprivation in 3T3-L1 cells. Based on the protein synthesis-dependent nature of transport elevation (31), the involvement of a novel protein in transport activation was suggested.

CHAPTER 4
EVIDENCE FOR PARTICIPATION OF A LABILE PROTEIN IN GLUCOSE TRANSPORT ACTIVATION

Introduction

Examples of changes in gene and protein expression in response to various conditions are replete in cell biology. In mammalian systems, this type of regulation has been studied extensively because cells exhibit the capacity to adjust to environmental conditions. Of the many signals to which cells are exposed, those that result from nutritional modifications comprise a large category. The control that nutrients have on their own regulation is of particular interest. The mechanisms underlying metabolic alterations in response to cholesterol and carbohydrate have been recently reviewed by Towle (19). Also, the area of transport has been studied extensively as it is limiting for the utilization of many nutrients (4;20). For example, amino acid deprivation has been shown to result in increased amino acid transport in liver and kidney cells (67;68). This phenomenon is similar in many respects to that of glucose transport activation observed in glucose-deprived 3T3-L1 cells under investigation here.

Glucose is the main energy source of most cells. The effect of this nutrient on gene and protein expression are broad areas of study. A review on glucose-stimulated genes by Mitanchez et al. (69) mentions many genes that encode for proteins involved in the metabolic pathways of glycolysis, fatty acid biosynthesis, and triglyceride synthesis, but emphasizes that the specific role of glucose can only be determined with cell culture systems. Two well-studied glucose-stimulated genes, L-type pyruvate kinase in the liver and Spot 14 in adipocytes, contain closely related response elements in their promoters, the glucose response element (GIRE) and carbohydrate response element (ChoRE), respectively. These elements bind proteins of the basic helix-loop-helix leucine zipper (b-HLH-LZ) family, which includes the c-*myc* oncogene product (19). Proteins which were originally discovered from their induction by glucose deprivation now comprise the stress-inducible family known as the GRPs, an acronym for Glucose-Regulated Proteins. CCAAT elements are implicated in the regulation of grp genes (70). The level of stress required to induce the GRPs leads to aberrant protein glycosylation and folding which differs from some of the other glucose deprivation-specific responses. Carlson et al. (71) found that glucose deprivation induces *gadd153* mRNA and protein while investigating the possibility that *gadd153* negatively regulates CCAAT/enhancer-binding protein (C/EBP) transcription factors. These authors also suggest that aberrant *gadd153* expression may play a part in the tumorigenesis of myxoid liposarcomas, an adipocyte tumor, through interference with normal C/EBP transcription factor function. A more direct correlation with cancer was made in another study, where Shim and colleagues (72) reported that glucose deprivation caused c-Myc transformed cells to undergo apoptosis while nontransformed cells arrested in the G_0/G_1 phase of the cell cycle(73). From these studies it is evident that glucose can affect expression of genes, mRNA, and proteins, which in turn can benefit or impair cells.

The results of the previous chapter suggest the involvement of a newly synthesized protein in the glucose deprivation-induced transport activation observed in 3T3-L1 adipocytes, in accordance with the protein synthesis-dependent nature of this phenomenon. Such a protein could function either by activating GLUT1 or by interrupting an association between the transporter and an inhibitor molecule. A similar argument has been made for amino acid deprivation (74). Also, Nicholson and McGivan (75) suggest that a protein is synthesized in amino acid-deprived renal epithelial cells which activates the excitatory amino acid carrier 1 (EAAC1)(68). New protein synthesis is also an adaptation of 3T3-L1 adipocytes to glucose deprivation. In this chapter, we investigate this adaptation in relation to transport, both indirectly and directly. Lysosomal protein degradation is inhibited and its effect on transport is measured. Transport is analyzed in response to glucose removal and refeeding with and without inhibition of protein synthesis. The effect of tunicamycin (which inhibits synthesis of N-linked glycosylated proteins) on glucose transport activation is considered. Finally, we attempt to visualize differences in proteins expressed in glucose-deprived versus control cells in specific subcellular fractions.

Results

Effect of Inhibitors of Protein Degradation on Glucose Transport in Control, Glucose-deprived, and Glucose-refed 3T3-L1 Adipocytes

The phenomenon of transport activation in response to glucose deprivation requires new protein synthesis, as discussed earlier. This prompted us to consider the role of protein degradation specifically in response to glucose readdition. The studies in this section sought to determine whether inhibitors of protein degradation would prevent "down-regulation" of glucose transport, defined as the return from the activated state to basal transport in response to glucose readdition. This down-regulation has been shown to occur by 4 hours (76). There are two general mechanisms for protein degradation in cells: the lysosomal pathway and the cytosolically based ubiquitin degradation pathway. Figure 4-1, which shows transport rates in glucose-deprived cells replenished with glucose, illustrates the effects of chloroquine, an inhibitor of lysosomal degradation, on glucose refeeding. First, this experiment clearly demonstrates that basal levels of glucose transport are restored after glucose is added back, as discussed above. This process follows first order kinetics, exhibiting a half-time of 1 hour. Rates were also measured in cells maintained in glucose-fed and glucose-deprived medium as controls. The small elevation in transport is seen in glucose-fed cells in response to chloroquine treatment which is reasonable if transporter degradation is inhibited. Indeed, this would therefore provide a positive control for the action of chloroquine. In fact, Ortiz et al. (49) demonstrated that GLUT1 is degraded in lysosomes in 3T3-C2 fibroblasts. However, chloroquine had no effect

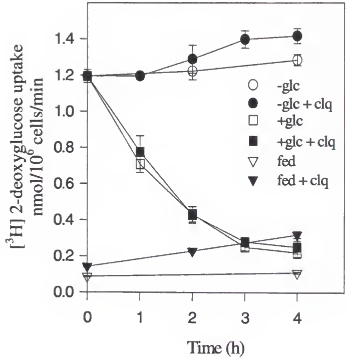

Figure 4-1 - Glucose Refeeding +/- Chloroquine 3T3-L1 Adipocytes were incubated for 18 hours in medium containing either 25 mM glucose (*fed*, inverted triangles) or 0 mM glucose (glucose-deprived, circles and squares). Chloroquine (*clq*, 50 µM) was added (filled symbols) at the last 30 minutes or 2 hours of incubation, or time -1/2 h or -2 h. Glucose (25 mM) was added back to one set of glucose-deprived cells (squares). Deoxyglucose transport was assayed at the indicated times from 0 to 4 hours after the incubation. The rates, expressed as nmol/10^6 cells/min + S.E., are for duplicate assays and are representative of two independent experiments.

(24) on the down-regulation induced with refeeding in 3T3-L1 adipocytes. These results indicate that upon glucose readdition, transport activity decreases by a mechanism which is not affected by inhibition of lysosomal degradation. If a protein responsible for the increase in glucose transport is degraded, it is not by a lysosomal pathway.

Response of Enhanced Transport Activity to Glucose Readdition in Glucose-deprived 3T3-L1 Adipocytes

In the previous chapter we demonstrated the 10-fold increase in the rate of glucose transport in glucose-deprived 3T3-L1 adipocytes compared to fed controls. We established that in these cells, unlike many other types, this is not a result of an increase in transporter at the cell surface. Yet, new protein synthesis is required for the increase in transport activity. Also, transport activation is rapidly reversed upon glucose refeeding. The mechanisms for this normalization depend upon the specific cell type (see Klip et al. (21). In this section, we have explored this reversal to examine the stability of potential regulators of transport activity.

In order to further describe the characteristics of the adaptation of 3T3-L1 adipocytes to glucose deprivation, we investigated the transport activation response in cells that were previously glucose-deprived. Figure 4-2A illustrates that the presence of cycloheximide abolishes the elevated glucose transport rate in glucose-deprived cells. This sensitivity to cycloheximide confirms the previously mentioned dependence on new protein synthesis. Also shown is the return to basal levels of transport after glucose refeeding for 4 hours, discussed in the previous section. The goal of this line of investigation was to determine whether there was any effect of prior glucose deprivation on the response of refed cells to re-deprivation. To this end, the rates of glucose transport were compared between control cells and refed cells with prior glucose deprivation (Figure 4-2B). Cells deprived of glucose for the first time are shown in the open and filled circles (with and without cycloheximide, respectively). In accordance with previous studies, these cells did not achieve maximal transport activity by 6 hours of glucose deprivation. Cycloheximide prevents this increase in transport. In contrast, the deprivation of cells previously glucose-deprived and then refed led to maximal transport activity within 6 hours. Such values are only observed after 12-18 hours in cells deprived of glucose for the first time. Interestingly, this accelerated response is sensitive to cycloheximide, as

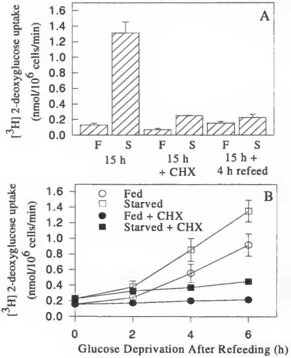

Figure 4-2 - Response of Enhanced Transport Activation to Glucose Readdition in Control and Glucose-deprived 3T3-L1 adipocytes *Panel A*, 3T3-L1 adipocytes in 35 mm plates were incubated in medium containing *(F)* 25 mm glucose (fed) or *(S)* 25 mm fructose (starved) in the absence or presence of cycloheximide *(CHX)*. Deoxyglucose transport was assayed for 10 minutes after 15 hours (+ and - CHX) or after 15 h plus a 4 hour incubation (-CHX) in fresh medium containing 25 mM glucose *(4h refeed)*. *Panel B*, Cells were fed (○, ●) or starved (□, ■) for 15 hours, refed for 4 hours, then starved again in the presence (●, ■) or absence (○, □) of CHX. Transport was assayed at the times indicated. The rates, reported as nmol/10^6 cells/min + S.E., are for duplicate assays and are representative of four independent experiments. The ○ vs □ data points were compared using Student's t test. The difference increases in significance: p = 0.01, 0.002, and 0.0003 for 2 hours, 4 hours and 6 hours, respectively.

Figure 4-2B shows. The requirement for newly synthesized protein for transport activation in previously glucose-deprived cells suggests fairly rapid turnover of the necessary protein(s).

Effect of Tunicamycin on Glucose Transport in Control and Glucose-deprived 3T3-L1 Adipocytes

We were interested in whether tunicamycin, an inhibitor of N-linked glycosylation, would affect glucose transport in the same fashion as does glucose deprivation. Figure 4-3 shows the results of 12 hours of tunicamycin treatment of control and glucose-deprived cells. The first four bars represent fed controls although they differ from each other by the inclusion of normal vs. dialyzed FBS (see legend). The FBS resulted in little difference. Therefore, the data points were combined to strengthen statistical analysis of the effect of tunicamycin. The mean ± S.E. ($n = 16$) for deoxyglucose uptake was 0.066 ± 0.006 and 0.050 ± 0.004 for fed without and with tunicamycin present, respectively. Thus transport activity in glucose-fed cells after 12 hours of tunicamycin treatment was reduced by 25% ($p = 0.02$). Figure 4-3 also shows that tunicamycin partially blocked the transport activation of glucose-deprived cells. In the absence of either fructose or glucose *(-glc)*, tunicamycin-treated cells transported deoxyglucose at a mean ± S.E. rate

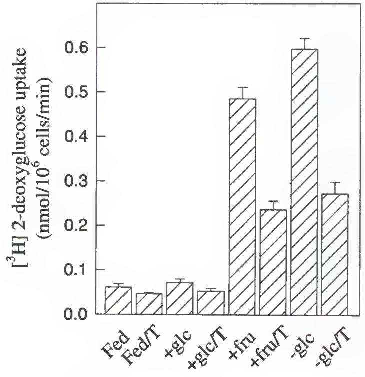

Figure 4-3 - Effect of Tunicamycin on Glucose Transport Activity in Glucose-fed and Glucose-deprived 3T3-L1 Adipocytes Cells in 35 mm plates were treated for 12 hours in complete DMEM supplemented with 10% FBS *(Fed)*, or glucose-free DMEM supplemented with 10% dialyzed FBS alone *(-glc)* or containing either 25 mM glucose *(+glc)* or 25 mM fructose *(+fru)*. Incubations were in the absence or presence of 2.5 μg/ml tunicamycin *(T)*. Deoxyglucose uptake was assayed and rates, expressed as nmol/10^6 cells/min ± S.E., are for duplicate assays and are representative of two independent experiments.

of 0.273 ± 0.026 nmol/10^6 cells/min. This was a 54.4% reduction ($p = 8.1 \times 10^{-6}$) from nontreated cells (0.597 ± 0.024). With fructose present (*+ fru)*, the mean ± S.E. transport rate was 0.485 ± 0.026. Tunicamycin treatment reduced this rate to 0.236 ± 0.020, a 51.3% loss of activity ($p = 2.6 \times 10^{-6}$). Thus in the presence or absence of fructose, tunicamycin reduced transport activity by approximately 50% in glucose-deprived cells. This might suggest that transport activation is in part mediated by a newly synthesized glycoprotein. This interpretation however is complicated by the fact that GLUT1 itself is glycosylated. Thus, tunicamycin could potentially affect the biosynthesis of the transporter independently of an activator.

This last possibility is explored in Figure 4-4. In this experiment glucose-fed cells were compared with glucose-deprived cells in the absence or presence of tunicamycin. A subfractionation of the cells was performed in order to monitor the subcellular localization of the unglycosylated form of GLUT1, which migrates at 36 kDa (77) in 3T3-L1 adipocytes. Figure 4-4 shows p36 in every fraction in both control and glucose-deprived cells, which suggests ongoing biosynthesis. The appearance of p36 in the plasma membrane fraction is important because this is the

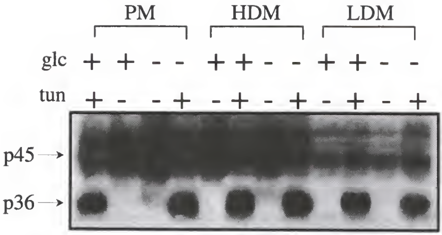

Figure 4-4 - Subfractionation of Glucose-fed versus Glucose-deprived +/- Tunicamycin-treated 3T3-L1 Adipocytes Cells were subfractionated as described in Materials and Methods after 12 hours in either glucose-free DMEM *(- glc,* see Figure 4-3 legend*)* or DMEM *(+ glc)* in the absence or presence of 2.5 μg/ml tunicamycin *(+* or *- tun)*. HDM, LDM, and PM fractions were loaded 50 μg per lane. GLUT1 was analyzed by immunoblotting with anti-GLUT1 using enhanced chemiluminescence. (Data generated by Joe Hwang, used by permission).

functional location of GLUT1. These data demonstrate that inhibition of glycosylation does not prevent GLUT1 targeting to the plasma membrane in 3T3-L1 adipocytes. Figure 4-4 also shows that at the plasma membrane, the level of p45 (the normal glycoform) decreases with the appearance of p36. The activity of p36, however, might not be the same as that of p45. Densitometric analysis of GLUT1 in the PM fraction was performed, shown in Figure 4-5.

A comparison of the intensity of p45 with and without tunicamycin in glucose-fed and glucose-deprived cells is illustrated in Figure 4-5A. In the presence of tunicamycin, the properly glycosylated GLUT1 was 39% of control in fed and 46% of control in glucose-deprived PMs. Panel B demonstrates that, when the intensity of the unglycosylated GLUT1 is added to that of the normal glycoform, the total is about 1.6 times that of GLUT1 in the absence of tunicamycin. Compared to the respective controls, the tunicamycin-treated total GLUT1 value was 164% for fed and 158% for glucose-deprived PMs. Therefore, with tunicamycin, there is a positive correlation between the loss of transport activity and the decrease in p45 intensity, despite the appearance of p36 in both fed and glucose-deprived plasma membranes. Taken together, Figures 4-4, and 4-5 suggest that glycosylation influences the activity of GLUT1. A study by Feugeas et al.(65)(78), in which human erythrocyte GLUT1 was

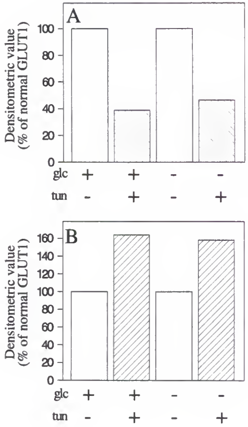

Figure 4-5 - Densitometric Analysis of Plasma Membrane Fractions from Figure 4-4 Arbitrary values for bands were obtained from a scanned image of the PM lanes in Figure 4-4, using the computer program NIH Image. The normal glycoform of GLUT1, p45, was scanned from the lanes representing tunicamycin-untreated *(- tun)* glucose-fed *(+glc)* and glucose-deprived *(-glc)* PM. The densitometric values for p45 in the *-tun* lanes were normalized to 100% (open bars). *(Panel A)* Values for p45 in the presence of tunicamycin are given as the percent of untreated for both control and glucose-deprived samples. *(Panel B)* Both p45 and p36 were quantitated from glucose-fed and glucose-deprived *+tun* lanes. The sum of the values from each is shown as the percentage of p45 from the respective normalized values.

reconstituted into proteoliposomes, gives precedence for this interpretation. These authors showed that treatment of the proteoliposomes with the deglycosylating enzyme N-glycanase reduced glucose transport by 50%.

Analysis of Proteins in Subcellular Fractions from Control and Glucose-deprived 3T3-L1 Adipocytes

Retention of transport activity in glucose-deprived plasma membrane vesicles (Chapter 3) and the evidence in this chapter suggesting the participation of a labile protein prompted a comparison of the protein composition between control and glucose-deprived cells. We began by looking at the PM fraction, which was investigated using two techniques. For one set of experiments, cell surface proteins were biotinylated as described in Materials and Methods. After cell surface biotinylation, cells were handled in four different ways. For one analysis, total membrane fractions were prepared from biotinylated cells and proteins separated on 2-D SDS-PAGE. In another, cell surface biotinylated proteins were isolated after membrane extraction by precipitation with streptavidin agarose. The streptavidin agarose-precipitated proteins were separated using 1-D SDS-PAGE. Alternatively, monomeric avidin was substituted for streptavidin-agarose for two-dimensional analysis of biotinylated proteins. Unlike streptavidin agarose, bound proteins can be released from monomeric avidin using 2 mM biotin. This allows proteins to be released from the avidin complex in a buffer that is amenable to subsequent isoelectric focusing. Finally, the subfractionation protocol was used to collect plasma membranes from previously cell-surface biotinylated control and glucose-deprived cells. GLUT1-containing vesicles were isolated from these plasma membranes using magnetic beads as described in Materials and Methods. The biotinylated proteins in these GLUT1-containing vesicles were analyzed on 1-D PAGE. In the molecular weight range analyzed, no reproducible differences were seen between cell surface proteins from glucose-fed and glucose-deprived cells using any of the above strategies.

Arguing that a newly synthesized protein(s) was involved in transport activation, we also examined plasma membrane proteins using metabolic labeling. After cells were labeled, the PM fractions from control and glucose-deprived cells were isolated as described in Materials and Methods and separated by 2-D SDS-PAGE. Again, no differences could be detected between control and glucose-deprived cells. In addition, we analyzed proteins in other subcellular fractions. These included the HDM, LDM, mitchondrial/nuclear, and cytosolic fractions. Again, we saw no reproducible differences in these samples in the molecular weight range tested.

Conclusions

The results in the previous chapter suggest the involvement of a newly synthesized protein in cellular adaptation to glucose deprivation. In this chapter, we provide additional evidence for such a protein. Figure 4-1 shows that transport activity quickly returns to normal with a half time of 1 hour. This could be due to *(I)* the specific glucose-mediated degradation of a protein involved in activation or *(ii)* dissociation of the protein from the transporter and/or the internalization of the protein. We examined the first hypothesis in Figure 4-1 which shows that loss of transport activity is not sensitive to lysosomal inhibition. Therefore, if the protein undergoes degradation, it is not through a lysosomal process. It is still possible that the activating protein exhibits rapid turnover. In metabolism, slowly degraded proteins are stable, often performing routine or basal functions. For example, GLUT1, a stable protein responsible for basal glucose transport in many cell types, has a half-life of 14-19 hours (77;79). GLUT1 has been shown to be degraded in lysosomes (24). On the other hand, rapidly degraded enzymes act at important points of control. This makes sense in the case of adaptation to glucose deprivation. Glucose utilization is a key point of metabolic control, and a protein(s) involved in emergency transport of this nutrient would not be required to be particularly stable. The chloroquine data in Figure 4-1 support this view, as lysosomal inhibitors do not affect degradation of abnormal or short-lived proteins.

If the second hypothesis mentioned above is true, then re-deprivation might lead to more rapid transport activation, which would be independent of protein synthesis. Figure 4-2 shows the test of this hypothesis. The dependence of glucose deprivation-enhanced glucose transport on protein synthesis is confirmed in Figure 4-2A. Figure 4-2B shows a difference in the kinetics of activation between newly glucose-deprived cells and those which were deprived, refed, and subsequently glucose-deprived. However, the re-deprived cells did not respond instantaneously as one might expect if a presynthesized and stored pool exists. Rather, the increase in transport was still gradual, reaching maximal rates approximately twice as fast as newly glucose-deprived cells. Further, this increase was sensitive to cycloheximide treatment which was not predicted with a pre-existing pool. In Figure 4-2 we show that transport activity, normalized by refeeding glucose-deprived cells, is once again sensitive to inhibition of protein synthesis when cells are subsequently glucose-deprived. This supports the idea that the protein is labile rather than internalized. Therefore, Figures 4-1 and 4-2 both present evidence of a protein that undergoes rapid turnover. However, we have not ruled out the possibility that the protein exists in a compartment that can no longer interact with the glucose transporter. The means of dissecting these responses requires observation and characterization of actual proteins which are glucose-dependent.

The tunicamycin experiments examine the participation of glycosylated proteins. The glycosylation of GLUT1 was important to consider when interpreting the data in Figure 4-3. The fact that the impairment of glucose transport activation was 50% complicated interpretation. We tested the possibility that tunicamycin prevents glycosylation of GLUT1 and thereby inhibits its functionality. Three lines of evidence supported this. First, tunicamycin reduced activation by 50%. Second, quantitation of the plasma membrane lanes in Figure 4-4, shown in Figure 4-5, demonstrates that tunicamycin treatment resulted in a p45 reduction of 60% in glucose-fed and 55% in glucose-deprived samples. The loss of the normal glycoform of GLUT1 during the 12 hour experiment approximates the predicted loss based on the known half-life. Third, we also show increases in p36 in both samples treated with tunicamycin, despite the loss of activity. Importantly, using the subfractionation methodology described in Chapter 3, Figure 4-4 demonstrates that unglycosylated GLUT1, p36, is targeted to the plasma membrane. If p36 is nonfunctional, this would explain the partial inhibition of transport activation seen in tunicamycin-treated cells. In a previous study, Feugeas et al. (78) reconstituted GLUT1 in proteoliposomes and showed that deglycosylation by N-glycanase treatment reduced transport activity by 50%. Only 50% of the GLUT1 was properly oriented after reconstitution, suggesting that the removal of oligosaccharide completely inhibits activity. Our studies, along with those of Feugeas et al (78) show evidence for the dependence of transport activity on glycosylation. Our results also imply that the postulated transport activating protein (TAP) is not affected by tunicamycin. This may mean that the TAP is not a glycoprotein or does not need the oligosaccharide for function.

The cell surface biotinylation and subfractionation procedures were utilized to examine proteins in plasma membranes and other subcellular fractions from glucose-fed and glucose-deprived cells. However, no unique proteins reproducibly appeared by these methods. The cell surface biotinylation approach was promising from the standpoint of examining plasma membrane proteins without intracellular contamination. A drawback, and perhaps the reason for the inability of these experiments to allow detection of reproducible differences between control and glucose-deprived samples, is that this technique selects a subset of proteins. That is, only proteins which have a primary amine available due to an exposed amino terminus or lysine residue are potentially visible with this technique. Although many biotinylated proteins were visualized, it is entirely feasible that proteins of interest were not within the range of experimental detection. Therefore, we chose to broaden the scope of our search for newly synthesized proteins by examining proteins in total membrane fractions and extending the molecular weight range chosen for analysis. The results are described in the next chapter.

CHAPTER 5
IDENTIFICATION AND CHARACTERIZATION OF GLUCOSE-DEPENDENT PROTEINS

Introduction

Previous experiments have shown that transport activation requires the synthesis of a new protein(s) which appears to be stable in the absence of glucose but turns over rapidly in the presence of glucose. The experiments in this chapter initially examine newly synthesized proteins in total membrane preparations from control and glucose-deprived cells. This fraction contains substantially greater amounts of protein in comparison to the subcellular fractions used in the previous experiments and thus increases the likelihood of detection. Any protein which is synthesized in response to glucose withdrawal is a potential candidate in transport activation specifically and/or the adaptation response in general. This membrane fraction was utilized previously in our laboratory to examine GLUT1 synthesis and turnover (77). In these experiments a number of proteins appeared to coprecipitate with GLUT1 in the 30-100 kDa molecular weight range. In this same molecular weight range, I looked for differences between newly synthesized proteins in total membrane fractions from glucose-fed and glucose-deprived cells which had been metabolically labeled. Using this approach, a 50 kDa protein was observed that was induced upon glucose deprivation. Sequence analysis of this protein, isolated from two-dimensional gels, resulted in matches for vimentin, an intermediate filament protein. With immunoblotting, the role of vimentin was examined to determine the nature (if any) of its glucose dependence. In the same 50 kDa "spot", we obtained sequence of a fragment that had no matches. With a portion of this sequence, we attempted to generate antiserum to this protein. Characterization of the 50 kDa protein was performed using subfractionation and membrane association experiments. These studies led to the identification of several other glucose-dependent proteins which, along with p50, were analyzed in refeeding experiments.

Results

Metabolically Labeled Membrane Proteins from Glucose-fed and Glucose-deprived 3T3-L1 Adipocytes

New protein synthesis was compared between total membrane fractions from glucose-fed and glucose-deprived cells using metabolic radiolabeling. This enabled us to visualize a larger subset of proteins than in earlier experiments. By examining the total membrane fraction, more of the cellular adaptation taking place was potentially observable. Separating proteins by two-dimensional gel electrophoresis, we observed a protein which was induced in glucose-deprived samples, appearing in the acidic region of the gel between the 45 kDa and 66 kDa molecular weight markers (Figure 5-1). Upon repeating this experiment, this range of the gel was expanded by allowing dye fronts to migrate off the gels, effectively separating the spots which appear in the area of interest (Figure 5-1, circle). This protein (pI ~5.2) was determined to have a molecular weight of 50 kDa by plotting the R_f (migration distance divided by the total distance of the dye front) of the protein standards against the log of the molecular weight and using the linear regression to calculate the unknown molecular

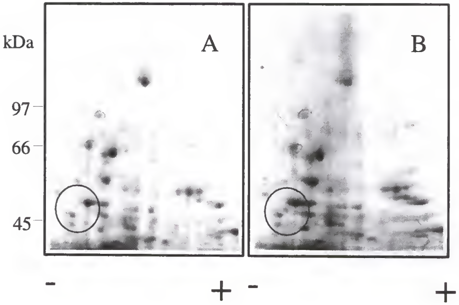

Figure 5-1 - Synthesis of Glucose-deprived vs. Fed Proteins
3T3-L1 Adipocytes were metabolically labeled and total membrane fractions analyzed by 2D SDS-PAGE followed by autoradiography as described in Materials and Methods. These results are representative of at least 5 independent experiments.

weight from its R_f. The 50kDa value represents the average from three independent experiments.

Protein patterns of 2D gels were easy to compare between glucose-fed and glucose-deprived samples and were reproducible over multiple experiments. The 50 kDa protein was carefully analyzed densitometrically by comparing it and a selected pattern of other metabolically labeled proteins between glucose-deprived and glucose-fed samples in different experiments. This normalizes any potential increase in specific activity of the methionine and cysteine pools in glucose-deprived cells. Therefore, a comparison of intensity was made between multiple proteins which allowed a more authentic representation of enhanced synthesis. An example of this is shown in Figures 5-2 and 5-3 and in Table 5-1. In Figure 5-2, 2D SDS-PAGE of metabolically labeled total membranes from control and glucose-deprived cells is shown. This is an independent experiment from Figure 5-1. Ten spots which migrate with the same pattern in each gel were chosen and numbered. In Figure 5-3, the spots are depicted with their given numbers, plotted using the coordinates assigned by the densitometer. Naturally, these coordinates will be similar but not identical based on the arbitrary nature by which autoradiographs are placed on the densitometer. Importantly, the patterns are superimposable.

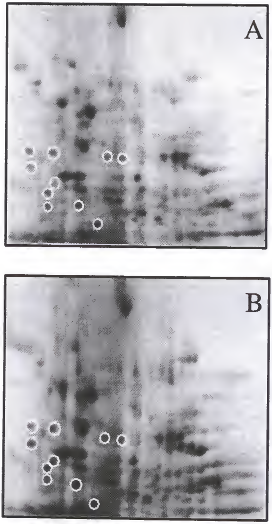

Figure 5-2 - Spots Selected for Densitometric Comparison
Total membrane fractions from metabolically labeled *(A)* glucose-fed and *(B)* glucose-deprived 3T3-L1 adipocytes were analyzed by 2D SDS-PAGE as in the experiment shown in Figure 5-1. Ten spots (circled) which migrated identically in both gels were selected for comparison of densitometric intensity.

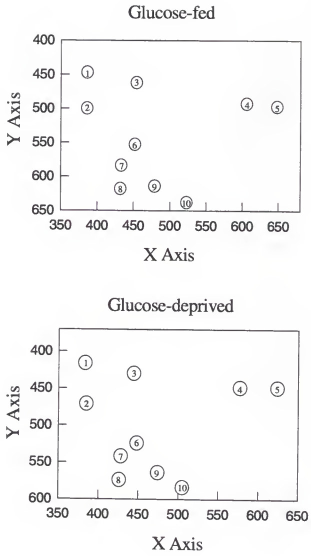

Glucose-fed

Glucose-deprived

Figure 5-3 - Assignment of Spots Selected for Densitometric Analysis The spots circled in Figure 5-2 are shown schematically, with the coordinates from densitometric analysis. The number assigned to each spot is depicted inside the representative symbol.

Table 5-1 - Comparison of Densitometric Values for Selected Spots

Spot Number	Fed	Starved	Ratio
1	0.034	0.047	1.382
2	0.130	0.163	1.254
3	0.209	0.195	0.933
4	0.146	0.448	3.068
5	0.127	0.197	1.551
6	0.022	0.244	11.091
7	0.433	0.635	1.467
8	0.385	0.564	1.465
9	0.211	0.104	0.493
10	0.408	1.431	3.507

Spots circled and numbered in Figures 5-2 and 5-3 were analyzed by densitometry. The arbitrary values assigned are given for the control *(Fed)* and glucose-deprived *(Starved)* spots, with the ratio of these values shown in the last column.

The densitometric values for the spots circled in Figure 5-2 are given in Table 5-1. A ratio was made of the densitometric values for the spots in glucose-deprived versus control samples, also given in Table 5-1. Spot number 6 had the highest ratio and is the 50 kDa protein shown in Figure 5-1. This type of analysis was repeated. Figure 5-4 shows that the 50 kDa spot of interest was reproducibly induced over other proteins. The mean induction of this spot under glucose deprivation was 10.6 ± 2.3 standard deviations. In light of this marked induction, this protein was viewed as a promising candidate for

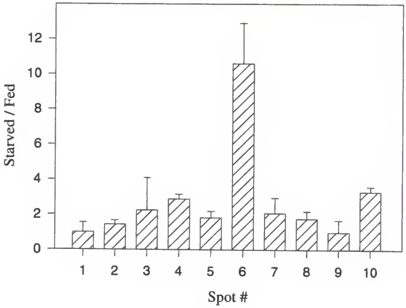

Figure 5-4 - Densitometric Ratio of Selected Spots Ten spots which were easily located in all 2D analyses of glucose-deprived and glucose-fed experiments were selected. Their densitometric values were measured as described in Materials and Methods. Ratios for glucose-deprived/glucose-fed were calculated and graphed here for each spot. For spots 1-5 and 7-10, n = 2. For spot 6, the 50 kDa spot highlighted in Figure 4-1, n = 3.

involvement in the adaptation of 3T3-L1 adipocytes to glucose deprivation.

Isolation, Concentration, and Microsequencing of a Glucose-dependent Membrane Protein

The 50 kDa glucose dependent protein discussed above was visible in gels stained with Coomassie Blue. The sensitivity of this protein stain is such that, generally, those bands or spots which Coomassie Blue stains are amenable to N-terminal sequencing. However, attempts at N-terminal sequence analysis of the 50 kDa protein were ambiguous at best, with results showing that very low concentrations of material was sequenced. The portion left over from sequencing was used for amino acid composition analysis. The results were compared against databases containing the amino acid composition of known proteins to search for matches. In addition, this provided information on the concentration of the analyzed material. Searches with the acquired amino acid composition data gave no matches with high scores: higher scores indicated a better probability of identity. Also, the concentration data demonstrated far higher concentrations than the amounts sequenced. We thus suspected that the protein was N-terminally blocked. To provide more data, internal sequencing was performed.

The technique of internal sequencing begins with an in-gel digest of the protein. This requires more starting material than does N-terminal sequencing, usually from 50 to 100 pmol. Protein was concentrated from 40 spots as delineated in Materials and Methods. This corresponded to more than 50 pmol, using values calculated from amino acid composition analyses on previous samples. Results from internal sequence analysis of this concentrated sample of the 50 kDa protein, carried out as described in Materials and Methods, were interesting. Three peaks from the HPLC profile of the in-gel EndoLys C digestion were chosen based on their mass spectra. Two of these peaks generated a total of three fragments. All three fragments, along with some less reliable data from N-terminal sequencing, matched the sequence of the intermediate filament protein, vimentin (Figure 5-5). The third peak resulted in sequence that had no matches on any protein database available on the Internet.

Immunoblotting Studies

We approached the disparate sequence data on the glucose-dependent 50 kDa protein from two angles. On one hand, we obtained antibodies to vimentin for use in immunoblotting experiments. Concurrently, we examined the non-matched sequence for a segment with antigenic potential

A.

QDLNMNYRGFX**ASYRSISRRTP**

B.

STRSVSSSSY RRMFGGSGTS SRPSSNRSYV TTSTRTYSLG
SALRPSTSRS LYSSSPGGAY VTRSSAVRLR SSVPGVRLLQ
DSVDFSLADA INTEFKNTRT NEKVELQELN DRFANYIDKV
RFLEQQNKIL LAELEQLKGQ GKSRLGDLYE EEMRELRRQV
DQLTNDKARV EVERDNLAED IMRLREKLQE EMLQREEAES
TLQSFRQDVD NASLARLDLE RKVESLQEEI AFLKKLHDEE
IQELQAQIQE QHVQIDVDVS KPDLTAALRD VRQQYESVAA
KNLQEAEEWY KSKFADLSEA ANRNNDALRQ AKQESNEYRR
QVQSLTCEVD ALKGTNESLE RQMREMEENF ALEAANYQDT
IGRLQDEIQN MKEEMARHLR EYQDLLNVKM ALDIEIATYR
KLLEGEESRI SLPLPTFSSL NLRETNLESL PLVDTHSKRT
LLIKTVETRD GQVINETSQH HDDLE

Figure 5-5 - Results of Sequence Analysis on 50 kDa Protein *Panel A*, Sequence from fragment of 50 kDa protein that had no matches (segment with good antigenicity in bold print). *Panel B*, Sequence of mouse vimentin with fragments sequenced from 50 kDa protein underlined.

The goal was to generate antiserum in order to directly test the properties of this protein.

Anti-vimentin studies

Anti-vimentin antibodies from various sources were tested on total membrane samples from adipocytes. We chose a rabbit anti-chicken vimentin antiserum (a gift from Dr. G. Bennett) for the majority of immunoblotting studies. This antibody recognized two species, the lower molecular weight of which was in the same range as the 50 kDa glucose-dependent protein (see Figure 5-6). Bands recognized by anti-vimentin from glucose-fed and glucose-deprived samples showed no change when compared on both 1D (see Figure 5-8, first two lanes) and 2D SDS-PAGE (data not shown). This indicates that vimentin is not the glucose-dependent protein under investigation but, due to similarity in pI and molecular weight, is likely contaminating the sample in total membrane preparations.

Peptide synthesis from glucose-dependent protein sequence data

The novel sequence fragment was analyzed for possible antigenicity. The C-terminal half (12-residues) was selected (see Figure 5-5) was chosen. The ATLAS database was searched for sequence matches not only on the entire 12 amino acid stretch but also 6 residues at a time. This was performed to be certain that an antibody generated against the whole fragment would not recognize a similar fragment from a potentially different "non-specific" protein. The ATLAS search returns exact matches with no gaps. This search verified that no known proteins of similar molecular weight and pI contained any of the sequence in this fragment. Therefore, the sequence was given to the University of Florida Protein Chemistry Core facility for peptide synthesis with instructions to add a cysteine residue to one end for coupling purposes. The result, Cys-Ala-Ser-Tyr-Arg-Ser-Ile-Ser-Arg-Arg-Thr-Pro-Asn, was of suitable purity for antigenic purposes and was water soluble. We then successfully coupled the peptide to Keyhole limpet hemocyanin and sent it to Cocalico Biologicals for antibody generation in rabbit. A dot blot of the first test bleed against the peptide was positive in contrast to a pre-immune bleed of the rabbit which did not recognize the peptide. However, the antiserum from the first and second test bleeds showed no reaction with proteins from total membrane samples separated by 1D SDS-PAGE (see discussion).

Membrane Association of Glucose-dependent Proteins

Taken together, the above studies suggest that the 50 kDa spot, examined because of its glucose responsiveness, was contaminated with the intermediate filament protein vimentin. The pI and molecular weight of vimentin closely match those of the spot which was analyzed. Also, vimentin is known to form filaments which surround lipid droplets in 3T3-L1 adipocytes (80). Such droplets are abundant in this cell type, making vimentin contamination in protein preparations a consideration. The presence of non-vimentin sequence (which also matched nothing else on protein database searches) implicates the presence of a separate protein. Vimentin was not induced in glucose-deprived samples (see Figure 5-8, first two lanes). Therefore, the unknown sequence is likely from the glucose responsive protein. Vimentin can be separated from many proteins using detergent. The experiments in this section aim to exploit this detergent extraction in the analysis of the glucose-dependent protein.

One-dimensional gel electrophoresis

The technique for isolating vimentin was utilized to determine if the glucose-dependent protein would colocalize with or be separated from vimentin. The nonionic detergent Triton X-100 (TX-100) was applied in a 0.5% PBS solution to intact cells. This treatment solubilizes certain proteins leaving vimentin and other insoluble proteins adhered to the plate. Using this approach, TX-100 soluble and insoluble proteins were separated. Samples from each were separated on 1D SDS-PAGE and immunoblotted with anti-vimentin. No

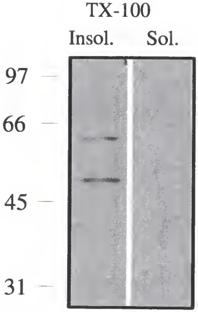

Figure 5-6 -Triton X-100 Extraction of 3T3-L1 Adipocytes
Cells were extracted as described in Materials and Methods. Samples of equal relative volume were resolved by 1D SDS-PAGE. Immunoblotting was carried out using rabbit anti-chicken anti-vimentin at a 1:10,000 dilution.

immunoreactive proteins were identified in the soluble fraction. The two vimentin bands (discussed above) were observed in the TX-100 insoluble fraction (Figure 5-6).

Two-dimensional gel electrophoresis

The above approach was also used to study glucose-fed and glucose-deprived samples by 2D SDS-PAGE. Instead of TX-100, Nonidet P-40 (NP40), another nonionic detergent, was used because of its application in the 2D protocol. NP40 compared favorably to TX-100 in that vimentin was separated from the soluble protein fraction (data not shown). Unfortunately, the 50 kDa protein also appeared in the insoluble fraction only. Unlike vimentin however, the 50 kDa protein was induced in the glucose-deprived sample over the control (Figure 5-7, short arrow). However these data suggest that the physical separation of these two proteins may prove arduous. Interestingly, Figure 5-7 shows another protein of lower molecular weight which also appears to respond to glucose deprivation (lower arrow). The molecular weight of this protein, determined as described previously for the 50 kDa protein, is 32 kDa, averaged from three fractions. Proteins in this molecular weight range were not analyzed in previous gels. Although it is possible that this protein is a degradation product of a larger protein, it is unlikely, as these extraction studies were performed

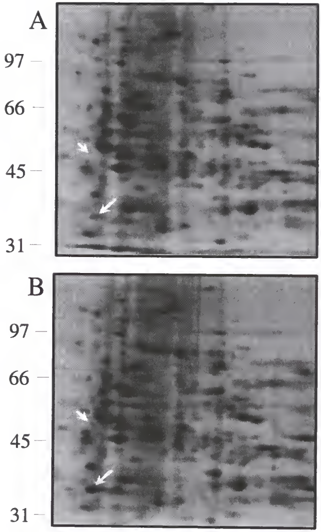

Figure 5-7 - NP40 Insoluble Fraction from Metabolically Labeled 3T3-L1 Adipocytes Cells were extracted as described in Materials and Methods. Samples of NP40 insoluble fractions, representing equal radioactivity, from *(Panel A)* glucose-fed cells and *(Panel B)* glucose-deprived cells were resolved by 2D SDS-PAGE. The small, upper arrow highlights the 50 kDa glucose responsive protein and the larger arrow below points to the 32 kDa glucose responsive protein.

in the presence of proteinase inhibitors (see Materials and Methods). In the following sections, we utilize tools already at hand to attempt further characterization of these glucose-dependent proteins, examining both glucose responsiveness and membrane localization.

Effect of Glucose Refeeding on Glucose-dependent Proteins

In this section, we examined whether the glucose-dependent proteins responded to glucose refeeding in a similar manner to transport activation. Using both anti-vimentin immunoblotting and metabolic radiolabeling, glucose-fed and glucose-deprived cells were compared with cells that were glucose-deprived then refed. Recall from the previous chapter that glucose-deprived cells are normalized with the readdition of glucose. The purpose of this experiment was to identify whether either of the proteins which are induced upon glucose deprivation are down-regulated with glucose refeeding. With immunoblotting of electrotransferred 1D SDS-PAGE, vimentin was observed to undergo no change (Figure 5-8, first two lanes). In contrast, the metabolically labeled 50 kDa protein was enhanced in the glucose-deprived sample, but not in the fed controls or the sample that was glucose-deprived then refed

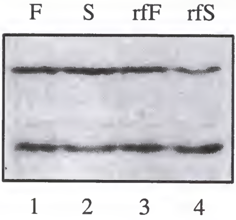

Figure 5-8 - Anti-vimentin Immunoblot on NP40 Insoluble Fraction from 3T3-L1 Adipocytes Cells were incubated in complete or glucose-free DMEM either for 24 hours only *(F* and *S,* respectively*)* or for an additional 24 hours of refeeding *(rf)* in complete DMEM *(rfF* and *rfS*, respectively). Cells were then extracted as described in Materials and Methods. Samples of equal volume were resolved by 1D SDS-PAGE. Immunoblotting was carried out using rabbit anti-chicken anti-vimentin at a 1:5,000 dilution. These results are representative or two separate experiments.

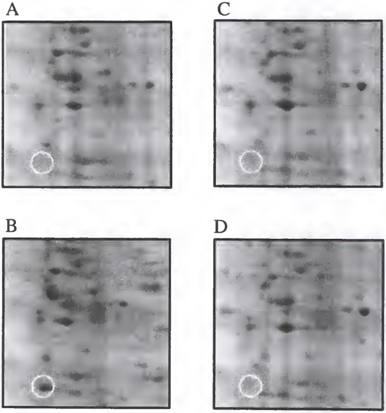

Figure 5-9 - NP40 Insoluble Fraction from Metabolically labeled Glucose-fed, Glucose-deprived, and Glucose-refed 3T3-L1 Adipocytes Cells were treated as described for Figure 5-8, metabolically labeled and resolved by 2D SDS-PAGE. *Panels A-D* are treated as lanes 1-4 in Figure 5-8. The area of the gels shown is the lower molecular weight, acidic region, with the 32 kDa protein highlighted.

(data not shown). The same result was observed with the 32 kDa protein, but in a more pronounced manner (Figure 5-9).

Subcellular Localization of Glucose-dependent Proteins

Glucose-fed and glucose-deprived cells were metabolically labeled, subfractionated, and analyzed by 2D SDS-PAGE. Each fraction was examined for appearance of glucose-dependent proteins. Again, the 50 kDa protein was not readily localized to any of the fractions examined, which corroborates our earlier experiments (see Chapter 4). However, the 32 kDa glucose-dependent protein was localized to the plasma membrane (Figure 5-10).

Conclusions

Two-dimensional gel electrophoresis was used to analyze newly synthesized, metabolically labeled membrane proteins in glucose-deprived versus control cells. A promising candidate which underwent 10-fold induction upon glucose deprivation (as does transport activity) was observed (Figures 5-1 - 5-4). We then isolated this protein from multiple two-dimensional gels for further study. Internal sequence analysis resulted in a match with vimentin and a fragment which matched nothing in the protein databases

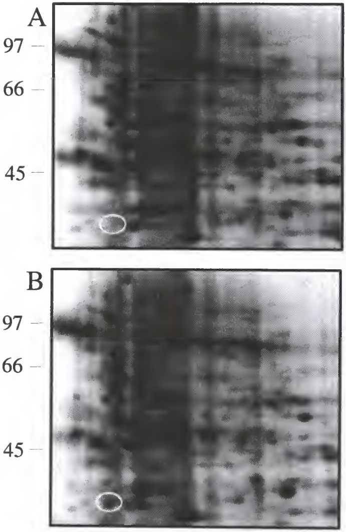

Figure 5-10 - Plasma Membrane Fraction of Glucose-fed and Glucose-deprived Metabolically Labeled 3T3-L1 Adipocytes Metabolically labeled cells were subfractionated as described in Materials and Methods. Plasma membrane fractions from *(Panel A)* glucose-fed and *(Panel B)* glucose-deprived cells were resolved by 2D SDS-PAGE. The 32 kDa glucose dependent protein is circled.

available on the Internet (Figure 5-5). We attempted to further characterize this protein by generating antiserum against an antigenic portion of the novel fragment. Although this anti-peptide antiserum recognized the peptide, it failed to react with any bands from total membrane samples. This could be due to the unavailability of this fragment for antibody interaction in the protein as it migrates on the gel system employed. For example, the region of the protein containing the fragment may be buried or masked by SDS. Performing either native gels or a mild proteolytic treatment of the gel may expose the fragment. Immunoblotting such gels with the anti-peptide antiserum could then help to determine whether masking took place. Vimentin is a well characterized protein belonging to the family of intermediate filament proteins. We thus made use of available anti-vimentin antibodies in immunoblotting studies (Figures 5-6 and 5-8). Along with radiolabeling data (Figure 5-7), these studies indicated that the glucose dependent protein is not vimentin. Taken together, the sequencing and immunoblotting data suggest a novel glucose-dependent protein which is contaminated by vimentin. Our sequence-to-antibody approach allowed us to recognize contamination of the spot of interest with vimentin, an abundant protein in 3T3-L1 adipocytes (80).

In light of the problem of vimentin contamination, it was of interest to determine whether the 50kDa protein would be solubilized in nonionic detergent or remain insoluble as does vimentin (Figure 5-6). If soluble, this would be an effective means of removing the protein from the abundant filamentous protein. However, the 50 kDa protein was NP40-insoluble, like vimentin (Figure 5-7). Unlike vimentin, it responded to glucose deprivation. In this experiment, we also noted a previously undetected protein with a molecular weight of 32 kDa (Figure 5-7). Previous experiments did not examine this molecular weight range thus the oversight. This protein also was induced by glucose deprivation. In addition, refeeding glucose-deprived samples resulted in the reduction of the 32 kDa protein (Figure 5-9). Another intriguing observation was the localization of this protein to the plasma membrane fraction (Figure 5-10).

In this chapter we describe a method for analyzing newly synthesized proteins from total membrane fractions of glucose-fed and glucose-deprived cells. We demonstrate the appearance of two glucose-dependent proteins of 50 kDa and 32 kDa. Both are appealing from the standpoint of the adaptation of 3T3-L1 cells to glucose deprivation. Data presented in this chapter provide groundwork for linking these proteins to glucose deprivation-induced transport activation. Of course, demonstration of involvement requires further studies. These proteins represent one of the interesting future directions for this work, discussed in the following chapter.

CHAPTER 6
CONCLUSIONS AND FUTURE DIRECTIONS

Conclusions

This work examined glucose deprivation and the manner in which cells respond to this challenge. Many different cell types are known to exhibit enhanced glucose transport under conditions of glucose deprivation. I focused on this global and physiologically relevant response and on proteins which may be involved. While the mechanisms by which cells increase transport activity are cell-type specific, the emphasis of this thesis has been the adipocyte model system, the 3T3-L1 cell line, in which this mechanism is unknown. However, in appendix I, I also presented studies performed in human pulmonary aortic endothelial (HPAE) cells. These studies were done in collaboration with Dr. Gary Visner, Department of Pediatrics (University of Florida). The HPAE studies describe, for the first time, the kinetics of glucose transport under normal and glucose-deprived conditions in these cells. In addition, the response of GLUT1 protein and mRNA was analyzed, as well as the general requirements for protein and mRNA synthesis. These studies reiterate the point that different cell types respond to glucose deprivation in distinct ways. I have demonstrated that in HPAE cells, glucose transport enhancement takes place via a change in both Vmax and Km. In contrast, only Vmax is increased in 3T3-L1 adipocytes. Other differences are pointed out in Appendix I. The glucose deprivation-induced increase in transport requires new protein synthesis in 3T3-L1 adipocytes (31-33). This dependence on protein, not unique to 3T3-L1 cells, was the central theme of this research.

In an examination of proteins required in response to glucose deprivation, the logical starting place was the point of entry for glucose. The family of proteins responsible for the facilitated transport of glucose into mammalian cells, known as GLUTs for glucose transporters, has been extensively characterized. 3T3-L1 adipocytes express two of the glucose transporters, GLUT1 and GLUT4. With insulin-induced enhanced transport, GLUT4 levels increase at the cell surface (9;10). Consequently, our first objective in this research was to determine whether levels of either GLUT1 or GLUT4 increase at the cell surface in response to glucose deprivation. To accomplish this, I developed a technique for the subcellular fractionation of 3T3-L1 adipocytes. This methodology allows effective isolation of specific membrane fractions from 3T3-L1 cells. With our new technique, we have shown that GLUT1 is the major transporter present at the cell surface in 3T3-L1 adipocytes and that its synthesis is not enhanced in response to glucose deprivation. We also established that translocation of GLUT1 does not account for elevated glucose transport. However, the protein synthesis-dependent nature of the increase in transport activity suggests the involvement of a novel protein(s) in transport activation, or more generally, in the adaptation of cells to glucose deprivation. We have provided evidence for this by showing a difference in transport activity between plasma membrane vesicles, isolated with the subfractionation technique, from glucose-fed and glucose-deprived cells. The glucose-deprived vesicles retain elevated transport activity in comparison to controls. With this in mind, having ruled out both a role for GLUT4 and the enhanced synthesis or translocation of GLUT1, we looked for further evidence of protein participation in glucose deprivation.

The next step in our strategy was to pursue both indirect and direct evidence of protein involvement in the response to glucose deprivation. We first approached this by investigating the role of protein degradation in enhanced glucose transport. We did this by examining the reversal of the activation response. The increase in glucose transport is normalized upon readdition of glucose (76). We demonstrated that chloroquine, a lysosomal degradation inhibitor, does not affect this process. Therefore, if protein degradation is involved, it does not take place via a lysosomal mechanism. There is evidence that GLUT1 is degraded by the lysosomal pathway (24). This evidence furthers the argument that a protein separate from the transporter is required in activation. Also, the lysosomal pathway is generally reserved for long-lived proteins such as GLUT1, not short-lived proteins like those involved in metabolic responses requiring rapid control. An example of the latter is the phenomenon under investigation here.

Glucose-deprived cells return to basal levels of transport, or become normalized, when glucose is added back. We compared transport activation in newly glucose-deprived cells and normalized cells, glucose-deprived for a second time. These “re-deprived” cells activated transport gradually, but reached maximal transport levels in half the time required by newly glucose-deprived cells. Cycloheximide blocked transport activation in re-deprived cells as in newly deprived cells. These data could indicate that the protein can no longer interact with the glucose transporter, perhaps as a result of compartmentalization.

However, taken together with the chloroquine data, the requirement for new protein synthesis in normalized cells indicated the involvement of a protein with rapid turnover.

We also deduced that it is unlikely that this protein would be glycosylated from experiments measuring glucose transport in the presence of the glycosylation inhibitor, tunicamycin. These experiments showed that after 12 hours of glucose deprivation in the presence of tunicamycin, transport activity was reduced by 50%. GLUT1 is a glycosylated protein with a half-life of 14-19 hours (77;79). We hypothesized that the loss of activity was due to loss of functional GLUT1. Based on its half-life we assumed that by 12 hours, about half of the normally glycosylated (functional) GLUT1 would remain in tunicamycin-treated cells, and unglycosylated (nonfunctional) GLUT1 would appear. Our results, which again utilized the subfractionation protocol, taken together with data on reconstituted GLUT1 from another group (78), supported this idea.

With considerable evidence for the participation of newly synthesized protein other than GLUT1 in the response of 3T3-L1 adipocytes to glucose deprivation, demonstration of the existence of such a protein was the next goal. Initially no reproducible proteins were detected to be induced by glucose deprivation in specific subcellular membrane fractions. This was likely a result of low protein content with these analyses. Turning to total membrane fractions to compensate, we observed newly synthesized proteins of 50 kDa and 32 kDa which are induced upon glucose deprivation. Both of these proteins are NP40-insoluble. Importantly, both are sensitive to both glucose-deprivation and glucose-refeeding, making both interesting for future study. The 50 kDa protein, however, migrates with vimentin on 2D SDS-PAGE. On the other hand, the 32 kDa protein is localized to the plasma membrane, making it an exciting prospect for involvement in transport activation. The studies presented here demonstrate the response of 3T3-L1 adipocytes to the specific condition of glucose withdrawal. Osmotic stress and carbohydrate starvation are protected against by the addition of fructose. Also, the duration of glucose deprivation was relatively short compared with other studies (31;32;36;77). The observation of few differences in protein expression between glucose-fed and glucose-deprived cells indicates a lack of general stress and emphasizes the importance of the proteins which appear. In Figure 6-1 we present a model which suggests activation of GLUT1 in response to glucose deprivation as a result of new protein synthesis.

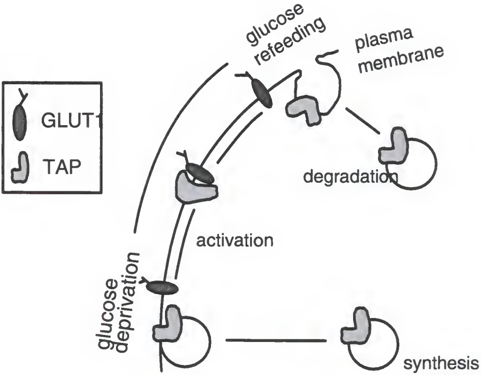

Figure 6-1 - Model of Response to Glucose Deprivation in 3T3-L1 Adipocytes The hypothetical transport activating protein *TAP*, is depicted as being synthesized in response to glucose withdrawal, interacting with GLUT1 and being degraded (not via lysosomes) upon re-addition of glucose. The 32 kDa protein, which is synthesized in response to glucose deprivation (see text) has been localized to the plasma membrane.

Future Directions

This research is primarily focused on the adaptation of 3T3-L1 adipocytes to glucose deprivation that results in enhanced glucose transport. New protein synthesis is a requirement for this phenomenon. We have established evidence that the newly synthesized protein is not GLUT1 or GLUT4. We also presented inhibitor studies which implicate protein involvement other than GLUT1 in transport activation. Further studies with other inhibitors could lend additional support to the protein degradation data. For example, lysosomal inhibitors which act via different mechanisms than chloroquine, which elevates intralysosomal pH, are available. Corroboration of one or more of these, such as proteinase inhibitors which include leupeptin and pepstatin, would strengthen the chloroquine data. Our arguments of a labile protein might be strengthened if similar experiments using an inhibitor of the ubiquitin-dependent degradation pathway, such as lactacystin, showed protection of enhanced transport with readdition of glucose. Preliminary experiments to these ends are shown in Appendix II.

With respect to our proposed mechanism for tunicamycin-induced reduction of transport activity, different approaches could corroborate the interpretation. The methodology of GLUT1 immunoprecipitation has been established in our laboratory (77). GLUT1 synthesis could be analyzed by pulse labeling glucose-fed and glucose-deprived cells for increasing times after 12 hours of treatment with or without tunicamycin, followed by immunoprecipitation, which would provide a series of "snap shots" of GLUT1. We would expect labeling experiments to show that p45 is not being synthesized in tunicamycin-treated samples and that p36 is, with little difference between control and glucose-deprived samples. Also, the half-time hypothesis could be verified by extending tunicamycin treatment to two half-times, with the expectation of observing complete inhibition of transport activation. However, as noted, strong support for our interpretation already exists (78).

Although the inhibitor studies provide indirect evidence for proteins involved in transport activation, direct evidence will come from studies on glucose dependent proteins. The further characterization of the glucose dependent proteins mentioned above is one future direction of this work. Generation of antiserum to one or both proteins will ameliorate numerous studies. Kinetic studies of appearance/disappearance of the glucose dependent protein(s) with respect to time and glucose concentration will be facilitated. For example, a glucose deprivation time course could be performed through 24 hours with 2 hour time points starting at zero glucose deprivation. At each time point, the detergent extraction which enriches the proteins of interest would be performed and the sample frozen and stored. All time points would be run side-by-side on 1D SDS-PAGE, followed by electrotransfer and immunoblotting. In such experiments, we would expect densitometric analysis to show up- and down-regulation of the glucose-dependent protein with glucose withdrawal and refeeding in a similar manner to glucose transport activity.

Finally, the interaction of the protein(s) with GLUT1 can be investigated. If the antiserum is suitable for immunofluorescence studies, colocalization of GLUT1 and the glucose dependent protein could be analyzed with this method. Alternatively, we have developed a technique combining magnetic bead immunoisolation with our subfractionation protocol. With this approach, we can determine whether the protein colocalizes with GLUT1 using antibody suitable for immunoblotting, which typically is not as stringent a requirement as for immunofluorescence. The

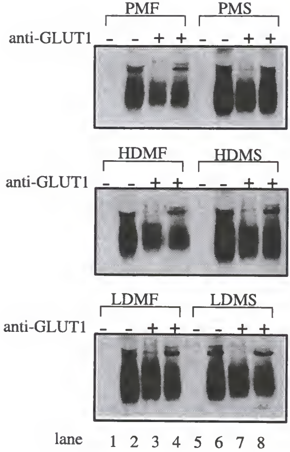
PMF
PMS
anti-GLUT1 - - + + - - + +
HDMF
HDMS
anti-GLUT1 - - + + - - + +
LDMF
LDMS
anti-GLUT1 - - + + - - + +
lane 1 2 3 4 5 6 7 8

Figure 6-2 - Isolation of GLUT1-containing Vesicles Using Magnetic beads GLUT1-containing vesicles were isolated from membrane fractions as described in Materials and methods and separated on 1D SDS-PAGE. GLUT1 was visualized by immunoblotting and enhanced chemiluminescence.

magnetic bead protocol, described in Materials and Methods, enables us to isolate GLUT1-containing vesicles from the membrane fractions, as shown in Figure 6-2. Antibodies to glucose-dependent proteins, once available, can be employed in immunoblotting studies on proteins isolated from GLUT1-containing vesicles. Another tact that might be taken with antibodies would be a test of whether antibody addition to cells inhibits transport activation by interfering with protein interaction. Lastly, antibodies could be useful in large-scale purification of the glucose-dependent proteins via affinity chromatography. Such preparations could be used in reconstitution studies similar to those of previous investigators (78;81), which would determine whether the glucose-dependent protein per se is capable of activating GLUT1 transport.

The identification of the proteins involved in glucose transport will help to understand the physiological regulation of glucose transport activity in response to hypo- and hyperglycemia. Also, recent studies have opened the glucose deprivation field to the study of cancer (71;73). Understanding the regulation of transport activity with respect to glucose deprivation potentially could have therapeutic consequences related to the control of tumorigenesis.

APPENDIX I

CHARACTERIZATION OF GLUCOSE TRANSPORT IN HUMAN PULMONARY AORTIC ENDOTHELIAL CELLS

A series of experiments which analyze glucose deprivation-induced enhanced glucose transport in human pulmonary aortic endothelial cells (HPAEs) is presented here. Few investigators have focused on the control of glucose transport in vascular endothelial cells and none in human endothelial cells. In these studies, done in collaboration with Dr Gary Visner, we examine the regulation of GLUT1, the "constitutive" transporter, in HPAEs by glucose. Specifically, glucose transport activity is quantitated in response to reduced glucose concentrations. GLUT1 protein and mRNA levels are analyzed under conditions of glucose deprivation. Also, the roles of protein and mRNA synthesis are considered in the response of HPAEs to glucose deprivation.

We demonstrate with these experiments that in HPAE cells, glucose-deprivation elicits a 4.5-fold increase in transport activity. This occurs via an approximately 2-fold increase in the Vmax and a 60% decrease in Km for glucose transport. In contrast to 3T3-L1 cells, where only Vmax changes, the mechanism behind transport enhancement in HPAEs also results in an increase in transporter affinity. We also show that the response requires both protein and mRNA synthesis. Finally, increased levels of GLUT1 protein and mRNA are detected in glucose deprived samples.

In Figure AI-1, glucose uptake in HPAEs was measured as a function of time. Transport is shown to be linear over 20 minutes. This result allowed us to proceed with glucose transport measurements with 10 minute uptake assays, as described in Materials and Methods. Figure AI-2 shows the results of a kinetic analysis on the HPAE cells. Panel B shows the Lineweaver-Burk plot of the data in Panel A. From this graph, the Km and Vmax were determined to be 0.46 mM and 2.11 nmol/10^6 cells/min, respectively.

Having determined that glucose transport could be measured in HPAEs, we next investigated the effect of glucose deprivation on the rate of uptake. Figure AI-3 shows the 4.5-fold increase in glucose uptake we observed upon 24 hours of glucose deprivation. This is a moderate effect in comparison to that seen in 3T3-L1 adipocytes. However, the rate change is considerable compared to the lack of a response noted in bovine vascular endothelial cells (23). This reiterates the point of cell type-specific mechanisms for response to glucose deprivation.

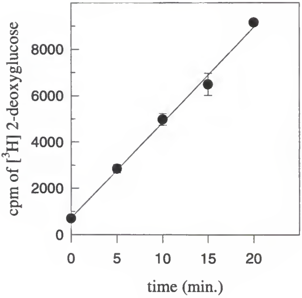

Figure AI-1 -Linearity of Glucose Uptake in Human Pulmonary Aortic Endothelial Cells HPAE cells in 35 mm plates were washed and incubated in KRP for 10 minutes. Transport of [^{3}H]2-deoxyglucose was assayed at the indicated time points. The counts per minute (cpm) of deoxyglucose uptake at each time point represents duplicate assays. Subsequent transport assays were performed at 10 minutes, within the linear range.

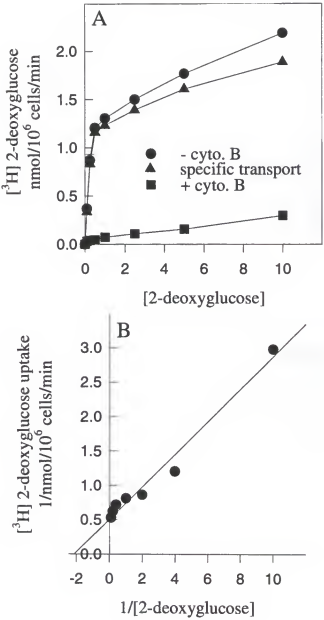

Figure AI-2 -Kinetics of Glucose Transport in HPAE Cells Kinetic analyses were performed as described in Materials and Methods. *Panel A*, a Michaelis Menten plot of specific glucose transport (shown as the difference between transport in the absence and presence of cytochalasin B). *Panel B*, Lineweaver-Burk plot of *A*. Km = 0.46 mM; Vmax = 2.11 nmol/10^6 cells/min.

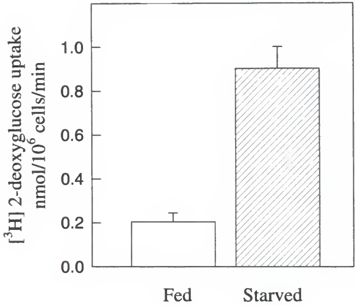

Figure AI-3 - Effect of Glucose Deprivation on Uptake of [^{3}H]2-deoxyglucose in Human Pulmonary Aortic Endothelial Cells HPAE cells were incubated in DMEM containing 25 mM *(Fed)* or 0 mM *(Starved)* glucose for 24 hours. Glucose transport was assayed as described in Materials and Methods. The data are reported as nmol/10^6 cells/min ± S.E. and represent n = 12.

To investigate the potential mechanism behind the glucose deprivation-induced 4.5-fold increase glucose transport in HPAEs we first measured the kinetics of glucose-fed and glucose-deprived cells to see observe the manner of the change. Figure AI-4 shows a representative graph of the Michaelis-Menten and Lineweaver-Burk plots for glucose-fed and glucose-deprived HPAEs. Tables AI-1 and AI-2 present the results of three different experiments. Different experiments represent different passage numbers of cells which may contribute to the discrepancy in the Vmax observed each time. The Km values remained relatively constant for the different experiments. To normalize the results, Table AI-2 shows the glucose-deprived/glucose-fed ratio for Vmax and Km values. The results indicate a 2.3-fold increase in Vmax accompanied by a 60% decrease in Km to correspond to the 4.5-fold increase in glucose transport. This observation is in contrast to the more often seen increase in Vmax with no change in Km with glucose deprivation. We determined the EC_{50} of glucose in HPAEs to be approximately 1 mM, as shown in Figure AI-5.

Finally, Figures AI-6 and AI-7 examine the role of protein and mRNA synthesis in glucose deprivation-enhanced glucose transport. We show in Figure AI-6 that inhibitors of both protein and mRNA synthesis result in prevention of

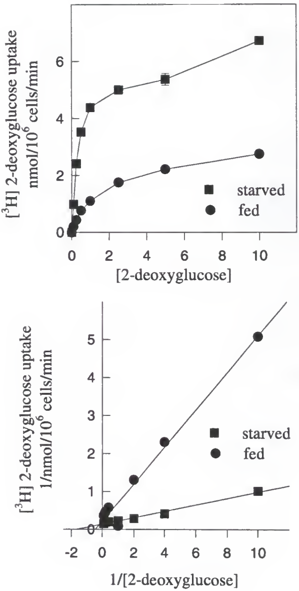

Figure AI-4 - Effect of Glucose Deprivation on Transport Kinetics in HPAE cells Kinetic analyses were performed as described in Materials and Methods on glucose-fed(circles) and glucose-deprived (squares) cells. This figure is representative of 3 different experiments. The Km and Vmax determinations follow in Table 1.

Table AI-1 - Effect of Glucose Deprivation on Transport Kinetics in HPAE Cells

Experiment	Km	Vmax	Glucose
1	1.26	2.67	Fed
	0.61	7.16	Deprived
2	1.55	0.57	Fed
	0.52	1.45	Deprived
3	1.69	2.85	Fed
	0.69	4.96	Deprived

Experiments were performed as described in Figure AI-4. Km and Vmax are reported as mM and nmol/10^6 cells/min, respectively.

Table AI-2 - Ratio of Glucose-deprived/Glucose-fed Km and Vmax Values from Table AI-1

Experiment	Glucose-deprived/Glucose-fed Ratio	
	Km	Vmax
1	0.48	2.68
2	0.34	2.54
3	0.41	1.74

The glucose-deprived to glucose-fed ratios for Km and Vmax values from the three experiments in Table 1 were determined. The mean ratio ± S.E. is 0.41 ± 0.04 for Km and 2.32 ±0.29 for Vmax. This indicates that in addition to a change in Vmax, glucose deprivation elicits a change transport affinity in HPAE cells.

enhanced transport. This suggests that new synthesis is required for both protein and mRNA. When analyzing GLUT1 however, a slight increase in mRNA level was observed. GLUT1 protein went up also and a lower molecular weight form appeared, presumably a result of aberrant glycosylation.

We show with these studies the examination of glucose transport and the effect of glucose deprivation in human pulmonary aortic endothelial cells. Although the relatively low magnitude of the response to glucose deprivation in HPAEs makes further study difficult, these results offer an interesting contrast to those observed in 3T3-L1 adipocytes and previously studied bovine vascular endothelial cells (23).

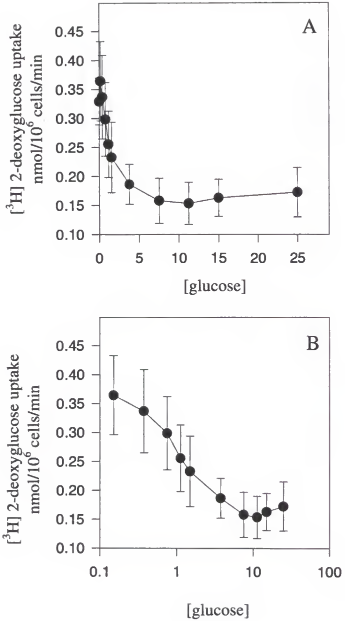

Figure AI-5 - Effect of Chronic Glucose on Transport in HPAEs Cells were incubated in DMEM containing increasing concentrations of glucose as described in Materials and Methods. Transport was assayed and is reported as nmol/10^6 cells/min ± S.E. This graph represents n = 4. The mean EC$_{50}$ from two independent experiments is 0.09 ± 0.01 mM.

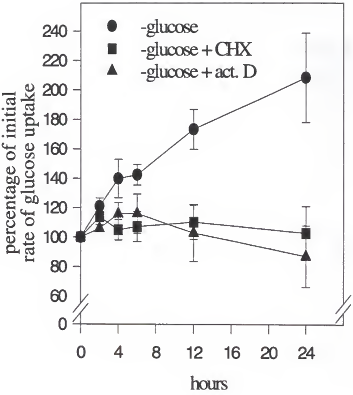

Figure AI-6 - Effect of Protein and mRNA Synthesis Inhibitors on Glucose Transport in HPAE Cells Cells were incubated for the indicated times in glucose-free DMEM alone or in the presence of either 20 µm cycloheximide or 24 nm actinomycin D. Transport was assayed at each time point, represented as the percentage of the initial rate of uptake. Data are combined from three independent experiments.

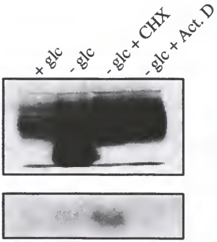

Figure AI-7 - Effect of Glucose Deprivation on Levels of GLUT1 protein and mRNA in HPAE Cells ± Cycloheximide or Actinomycin D Cells were glucose-fed *(+glc)* or glucose-deprived *(-glc)* ± either cycloheximide *(CHX)* or actinomycin D *(Act. D)* for 24 hours. *Above*, immunoblot of equal volumes of total membrane preparations, using anti-GLUT1 at 1:500 dilution. *Below*, northern analysis of samples, performed as described in Materials and Methods.

APPENDIX II
PRELIMINARY EXPERIMENTS

Other Inhibitors of Protein Degradation

Other inhibitors of protein degradation are available for our studies on the reversal of transport activation by glucose refeeding, as discussed in Chapter 6. In this section, preliminary experiments were performed using leupeptin and lactacystin. We have examined the effect of the weak base chloroquine, which elevates the pH and thus alters the physicochemical properties of lysosomes. Leupeptin, however, is a proteinase inhibitor. By specifically inhibiting trypsin-like and many cysteine proteinases, leupeptin is a significant inhibitor of lysosomal degradation. Obtaining results with another type of lysosomal degradation inhibitor will reinforce our conclusions. Also, with lactacystin, an inhibitor of the proteasome responsible for degradation of ubiquitinated proteins (82), we can test whether inhibition of rapid turnover affects the reversal of transport activation. The preliminary studies presented here, if verified, will lend more support to our hypothesis as they show *(I)* no affect with inhibition of lysosomal degradation and *(ii)* some protection from reversal with lactacystin, which might improve with higher concentrations or longer incubations.

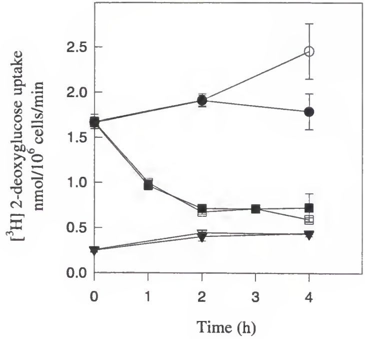

Figure AII -1 - Effect of Leupeptin on Reversal of Transport Activation in 3T3-L1 Adipocytes Transport was assayed on cells as in Figure 4-1, with 100 μM leupeptin added 2 hours prior to time zero.

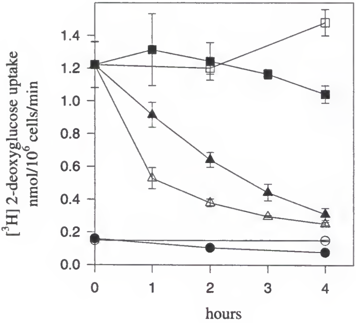

Figure AII-2 - Effect of Lactacystin on Reversal of Transport Activation in 3T3-L1 Adipocytes Transport was assayed as in the previous experiment, with 20 μM lactacystin added at 1 hour prior to time zero.

LIST OF REFERENCES

1 Voet, D. and Voet, J.G. (1995) *Biochemistry*, John Wiley & Sons, Inc.,

2 Walmsley, A.R. (1988) *TIBS* **13**, 226-231

3 Gould, G.W. and Bell, G.I. (1990) *TIBS* **15**, 17-23

4 Olson, A.L. and Pessin, J.E. (1996) *Annu.Rev.Nutr.* **16**, 235-256

5 Thomas, H.M., Brant, A.M., Colville, C.A., Seatter, M.J., and Gould, G.W. (1992) *Biochem.Soc.Trans.* **20**, 528-542

6 Baldwin, S.A., Baldwin, J.M., and Lienhard, G.E. (1982) *Biochem.* **21**, 3836-3842

7 Mueckler, M., Caruso, C., Baldwin, S.A., Panico, M., Blench, I., Morris, H.R., Allard, W.J., Lienhard, G.E., and Lodish, H. (1985) *Science* **229**, 941-945

8 Gould, G.W. and Holman, G.D. (1993) *Biochem.J.* **295**, 329-341

9 Cushman, S.W. and Wardzala, L.J. (1980) *J.Biol.Chem.* **255**, 4758-4762

10 Suzuki, K. and Kono, T. (1980) *Proc.Natl.Acad.Sci.USA* **77**, 2542-2545

11 James, D.E., Strube, M., and Mueckler, M. (1989) *Nature* **338**, 83-87

12 Birnbaum, M.J. (1989) *Cell* **57**, 305-315

13 Charron, M.J., Brosius, F.C., Alper, S.L., and Lodish, H.F. (1989) *Proc.Natl.Acad.Sci.USA* **86**, 2535-2539

14 Kaestner, K.H., Christy, R.J., McLenithan, J.C., Braiterman, L.T., Cornelius, P., Pekala, P.H., and Lane, M.D. (1989) *Proc.Natl.Acad.Sci.USA* **86**, 3150-3154

15 Fukumoto, J., Kayano, T., Buse, J.B., Edwards, Y., Pilch, P.F., Bell, G.I., and Seino, S. (1989) *J.Biol.Chem.* **264**, 7776-7779

16 Carruthers, A. (1990) *Physiol.Rev.* **70**, 1135-1176

17 McGowan, K.M., Long, S.D., and Pekala, P.H. (1995) *Pharmac.Ther.* **66**, 465-505

18 Widdas, W.F. (1988) *Biochim.Biophys.Acta* **947**, 385-404

19 Towle, H.C. (1995) *J.Biol.Chem.* **270**, 23235-23238

20 Malandro, M.S. and Kilberg, M.S. (1996) *Annu.Rev.Biochem.* **65**, 305-336

21 Klip, A., Tsakiridis, T., Marette, A., and Ortiz, P.A. (1994) *FASEB J.* **8**, 43-53

22 Haspel, H.C., Mynarcik, D.C., Ortiz, P.A., Honkanen, R.A., and Rosenfeld, M.G. (1991) *Molec.Endo.* **5**, 61-72

23 Kaiser, N., Sasson, S., Feener, E.P., Boukobza-Vardi, N., Higashi, S., Moller, D.E., Davidheiser, S., Przybylski, R.J., and King, G.L. (1993) *Diabetes* **42**, 80-89

24 Ortiz, P.A., Honkanen, R.A., Klingman, D.E., and Haspel, H.C. (1992) *Biochem.* **31**, 5386-5393

25 Walker, P.S., Ramlal, T., Donovan, J.A., Doering, T.P., Sandra, A., Klip, A., and Pessin, J.E. (1989) *J.Biol.Chem.* **264**, 6587-6595

26 Boado, R.J. and Pardridge, W.M. (1993) *J.Neurochem.* **60**, 2290-2296

27 Mayor, P., Maianu, L., and Garvey, W.T. (1992) *Diabetes* **41**, 274-285

28 Simmons, R.A., Flozak, A.S., and Ogata, E.S. (1993) *Endocrinology* **132**, 2312-2318

29 Blok, J., Gibbs, E.M., Lienhard, G.E., Slot, J.W., and Geuze, H.J. (1988) *J.Cell Biol.* **106**, 69-76

30 Green, H. and Kehinde, O. (1974) *Cell* **1**, 113-116

31 VanPutten, J.P.M. and Krans, H.M.J. (1985) *J.Biol.Chem.* **260**, 7996-8001

32 Reed, B.C., Shade, D., Alperovich, F., and Vang, M. (1990) *Arch.Biochem.Biophys.* **279**, 261-274

33 Tordjman, K.M., Leingang, K.A., and Mueckler, M. (1990) *Biochem.J.* **271**, 201-207

34 Yamada, K., Tillotson, L.G., and Isselbacher, K.J. (1983) *J.Biol.Chem.* **258**, 9786-9792

35 Walker, P.S., Donovan, J.A., VanNess, B.G., Fellows, R.E., and Pessin, J.E. (1988) *J.Biol.Chem.* **263**, 15594-15601

36 Kitzman, H.H., Jr., McMahon, R.J., Williams, M.G., and Frost, S.C. (1993) *J.Biol.Chem.* **268**, 1320-1325

37 Kozka, I.J., Clark, A.E., and Holman, G.D. (1991) *J.Biol.Chem.* **266**, 11726-11731

38 Williams, K.A. and Deber, C.M. (1991) *Biochem.* **30**, 8919-8923

39 Tamori, Y., Hashiramoto, M., Clark, A.E., Mori, H., Muraoka, A., Kadowaki, T., Holman, G.D., and Kasuga, M. (1994) *J.Biol.Chem.* **269**, 2982-2986

40 Mori, H., Hashiramoto, M., Clark, A.E., Yang, J., Muraoka, A., Tamori, Y., Kasuga, M., and Holman, G.D. (1994) *J.Biol.Chem.* **269**, 11578-11583

41 Lipmann, F. and Lee, S.G. (1978) in *Microenvironments and Metabolic Compartmentation* (Srere, P. and Estabrook, R.N., eds) pp. 263-281, Academic Press, New York

42 Flocco, M.M. and Mowbray, S.L. (1994) *J.Biol.Chem.* **269**, 8931-8936

43 Oxcan, S., Dover, J., Rosenwald, A.G., Wolfl, S., and Johnston, M. (1996) *Proc.Natl.Acad.Sci.USA* **93**, 12428-12432

44 Lachaal, M., Berenski, C.J., Kim, J., and Jung, C.Y. (1990) *J.Biol.Chem.* **265**, 15449-15454

45 Lachaal, M. and Jung, C.Y. (1993) *J.Cell.Physiol.* **156**, 326-332

46 Veyhl, M., Spangenberg, J., Puschel, B., Poppe, R., Dekel, C., Fritzsch, G., Haase, W., and Koepsell, H. (1993) *J.Biol.Chem.* **268**, 25041-25053

47 Mastick, C.C., Aebersold, R., and Lienhard, G.E. (1994) *J.Biol.Chem.* **269**, 6089-6092

48 Kandror, K. and Pilch, P.F. (1994) *J.Biol.Chem.* **269**, 138-142

49 Kandror, K.V. and Pilch, P.F. (1994) *Proc.Natl.Acad.Sci.USA* **91**, 8017-8021

50 Kandror, K.V., Yu, L., and Pilch, P.F. (1994) *J.Biol.Chem.* **269**, 30777-30780

51 Dulbecco, R. and Freeman, G. (1959) *Virology* **8**, 396-397

52 Frost, S.C. and Lane, M.D. (1985) *J.Biol.Chem.* **260**, 2646-2652

53 Fisher, M.D. and Frost, S.C. (1996) *J.Biol.Chem.* **271**, 11806-11809

54 Weber, T.M., Joost, H.-G., Simpson, I.A., and Cushman, S.W. (1988) in *Receptor Biochemistry and Methodology (The Insulin Receptor)* (Kahn, R.C. and Harrison, L.C., eds) pp. 171-187, Alan R. Liss, Inc., New York

55 Balch, W.E. and Rothman, J.E. (1985) *Arch.Biochem.Biophys.* **240**, 413-425

56 Markwell, M.A.K., Haas, S.M., Lieber, L.L., and Tolbert, N.E. (1978) *Anal.Biochem.* **87** , 206-210

57 Lowry, O.H., Rosenbrough, N.J., Farr, A.L., and Randall, R.J. (1951) *J.Biol.Chem.* **193** , 265-270

58 Laemmli, U.K. (1970) *Nature* **227**, 680-685

59 Semple-Rowland, S.L., Adamus, G., Cohen, R.J., and Ulshafer, R.J. (1991) *Electrophoresis* **12**, 307-312

60 Clancy, B.M. and Czech, M.P. (1990) *J.Biol.Chem.* **265**, 12434-12443

61 Fisher, M.D. and Frost, S.C. (1997) *Anal.Biochem.* **251**, 125-126

62 Walker, P.S., Ramlal, T., Sarabia, V., Koivisto, U.-M., Bilan, P.J., Pessin, J.E., and Klip, A. (1990) *J.Biol.Chem.* **265**, 1516-1523

63 Haspel, H.C., Wilk, E.W., Birnbaum, M.J., Cushman, S.W., and Rosen, O.M. (1986) *J.Biol.Chem.* **261**, 6778-6789

64 James, D.E., Piper, R.C., and Slot, J.W. (1993) *J.Cell Sci.* **104**, 607-612

65 Yang, J., Clark, A.E., Kozka, I.J., Cushman, S.W., and Holman, G.D. (1992) *J.Biol.Chem.* **267**, 10393-10399

66 Calderhead, D.M., Kitagawa, K., Tanner, L.I., Holman, G.D., and Lienhard, G.E. (1990) *J.Biol.Chem.* **265**, 13800-13808

67 Kilberg, M.S. (1986) *TIBS* **11**, 183-186

68 Mistry, A.M., Swick, A.G., and Romsos, D.R. (1997) *J.Nutr.* **127**, 2065-2072

69 Mitanchez, D., Doiron, B., Chen, R., and Kahn, A. (1997) *Endocrine Reviews* **18**, 520-540

70 Lee, A.S. (1992) *Curr.Opin.Cell Biol.* **4**, 267-273

71 Carlson, S.G., Fawcett, T.W., Bartlett, J.D., Bernier, M., and Holbrook, N.J. (1993) *Molec.Cell.Biol.* **13**, 4736-4744

72 Shim, H., Chun, Y.S., Lewis, B.C., and Dang, C.V. (1998) *Proc.Natl.Acad.Sci.USA* **95**, 1511-1516

73 Bray, G. and Bouchard, C. (1997) *FASEB J.* **11**, 937-945

74 Barber, E.F., Handlogten, M.E., and Kilberg, M.S. (1993) *J.Biol.Chem.* **258**, 11851-11855

75 Nicholson, B. and McGivan, J.D. (1996) *J.Biol.Chem.* **271**, 12159-12164

76 Kitzman, H. H., Jr. (1995) Dissertation, University of Florida.

77 McMahon, R. J. (1995) Dissertation, University of Florida.

78 Feugeas, J.-P., Neel, D., Pavia, A.A., Laham, A., Goussault, Y., and Derappe, C. (1990) *Biochim.Biophys.Acta* **1030**, 60-64

79 Sargeant, R.J. and Paquet, M.R. (1993) *Biochem.J.* **290**, 913-919

80 Lieber, J.G. and Evans, R.M. (1996) *J.Cell Sci.* **109**, 3047-3058

81 Carter-Su, C., Pillion, D.J., and Czech, M.P. (1980) *Biochem.* **19**, 2385-2390

82 Fenteany, G., Standaert, R.F., Lane, W.S., Choi, S., Corey, E.J., and Schreiber, S.L. (1995) *Science* **268**, 726-731

BIOGRAPHICAL SKETCH

Maxine Fisher was born in Bedford, England, on November 18, 1970. In 1983, her parents and youngest brother moved to Miami, Florida. Maxine attended the University of Miami and graduated with a bachelor's degree in chemistry, certified by the American Chemical Society. She then joined the Biochemistry and Molecular Biology Department at the University of Florida and worked under the supervision of Dr. Susan Frost. After graduation, Maxine plans to join the lab of Dr. Joel Goodman at the University of Texas Southwestern Medical Center in Dallas for postdoctoral training. There she will study protein sorting in yeast peroxisomes.

I certify that I have read this study and that in my opinion it conforms to acceptable standards of scholarly presentation and is fully adequate, in scope and quality, as a dissertation for the degree of Doctor of Philosophy.

Susan C. Frost
Susan C. Frost, Chair
Associate Professor of
Biochemistry and
Molecular Biology

I certify that I have read this study and that in my opinion it conforms to acceptable standards of scholarly presentation and is fully adequate, in scope and quality, as a dissertation for the degree of Doctor of Philosophy.

Daniel Purich
Daniel Purich
Professor of Biochemistry
and Molecular Biology

I certify that I have read this study and that in my opinion it conforms to acceptable standards of scholarly presentation and is fully adequate, in scope and quality, as a dissertation for the degree of Doctor of Philosophy.

Michael S Kilberg
Michael Kilberg
Professor of Biochemistry
and Molecular Biology

I certify that I have read this study and that in my opinion it conforms to acceptable standards of scholarly presentation and is fully adequate, in scope and quality, as a dissertation for the degree of Doctor of Philosophy.

Brian Cain
Brian Cain
Associate Professor of
Biochemistry and
Molecular Biology

I certify that I have read this study and that in my opinion it conforms to acceptable standards of scholarly presentation and is fully adequate, in scope and quality, as a dissertation for the degree of Doctor of Philosophy.

Bruce R Stevens
Bruce Stevens
Professor of Physiology

This dissertation was submitted to the Graduate Faculty of the College of Education and to the Graduate School and was accepted as partial fulfillment of the requirements for the degree of Doctor of Philosophy.

May, 1998

Robert T. Watson for KB

Dean, College of Medicine

Karen A. Holbrook

Dean, Graduate School